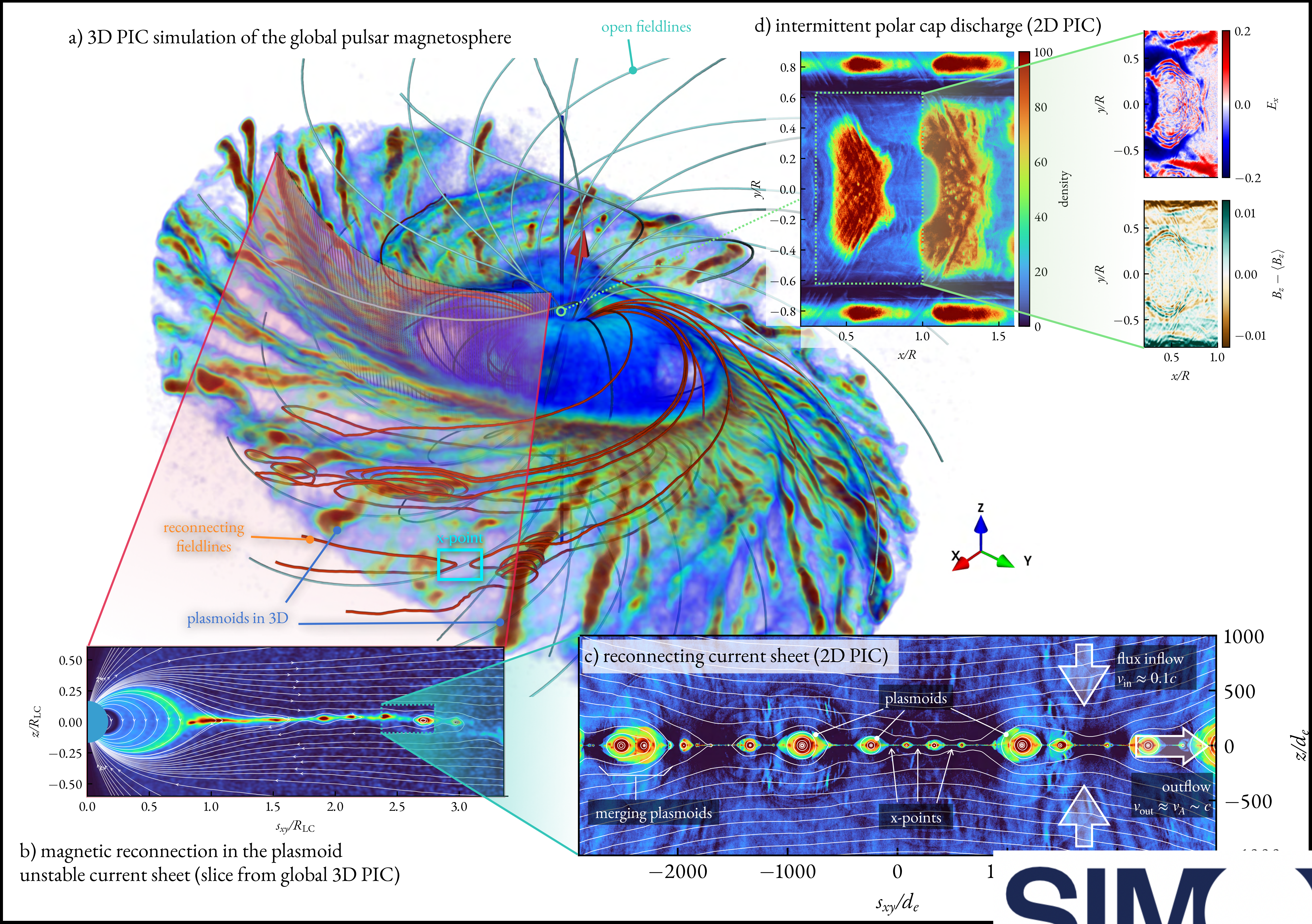

Pulsar magnetospheres and their radiation

Sasha Philippov (Maryland)

with:

Benoit Cerutti (*Grenoble*)
Sasha Chernoglazov (*Maryland*)
Sam Gralla (*Arizona*)
Hayk Hakobyan *(Columbia)*
Anatoly Spitkovsky (*Princeton*)
Andrey Timokhin (*Zielona Gora*)
Libby Tolman *(IAS, Flatiron)*
Dmitri Uzdensky (*Colorado*)

Philippov & Kramer, 2022, Annual Reviews of Astronomy & Astrophysics

SIMONS FOUNDATION
SCEECS
NSF

What is a pulsar?

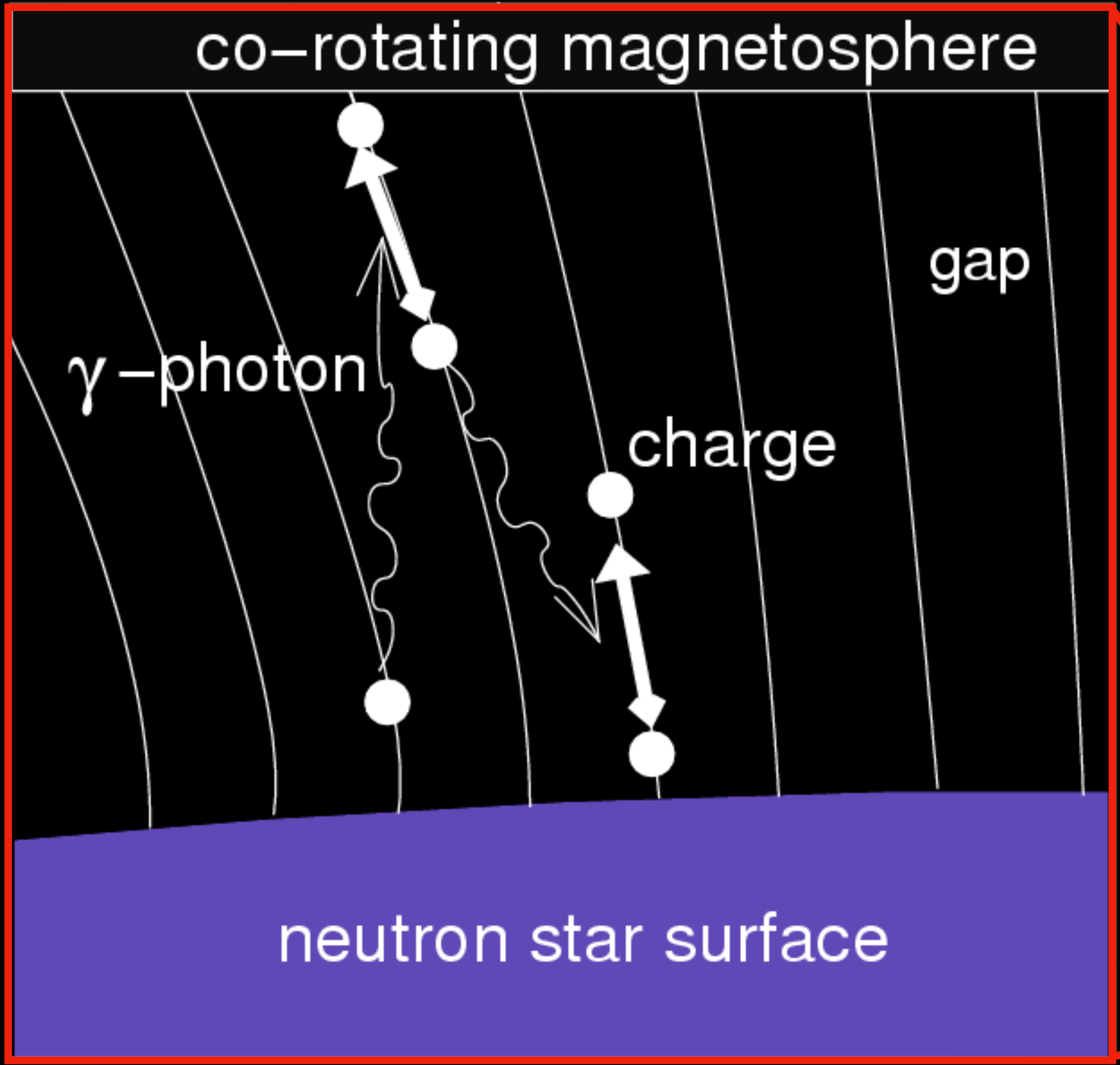

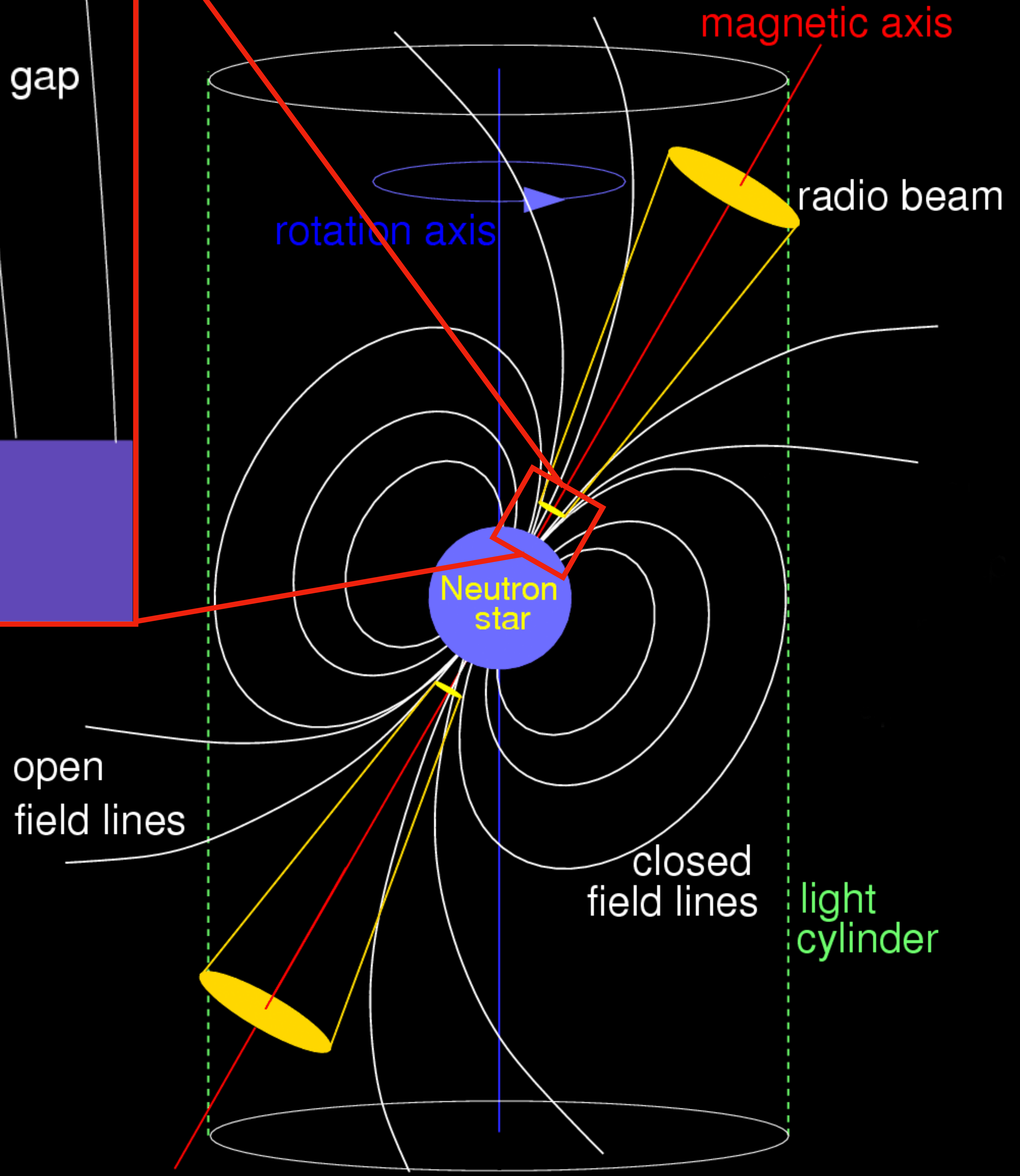

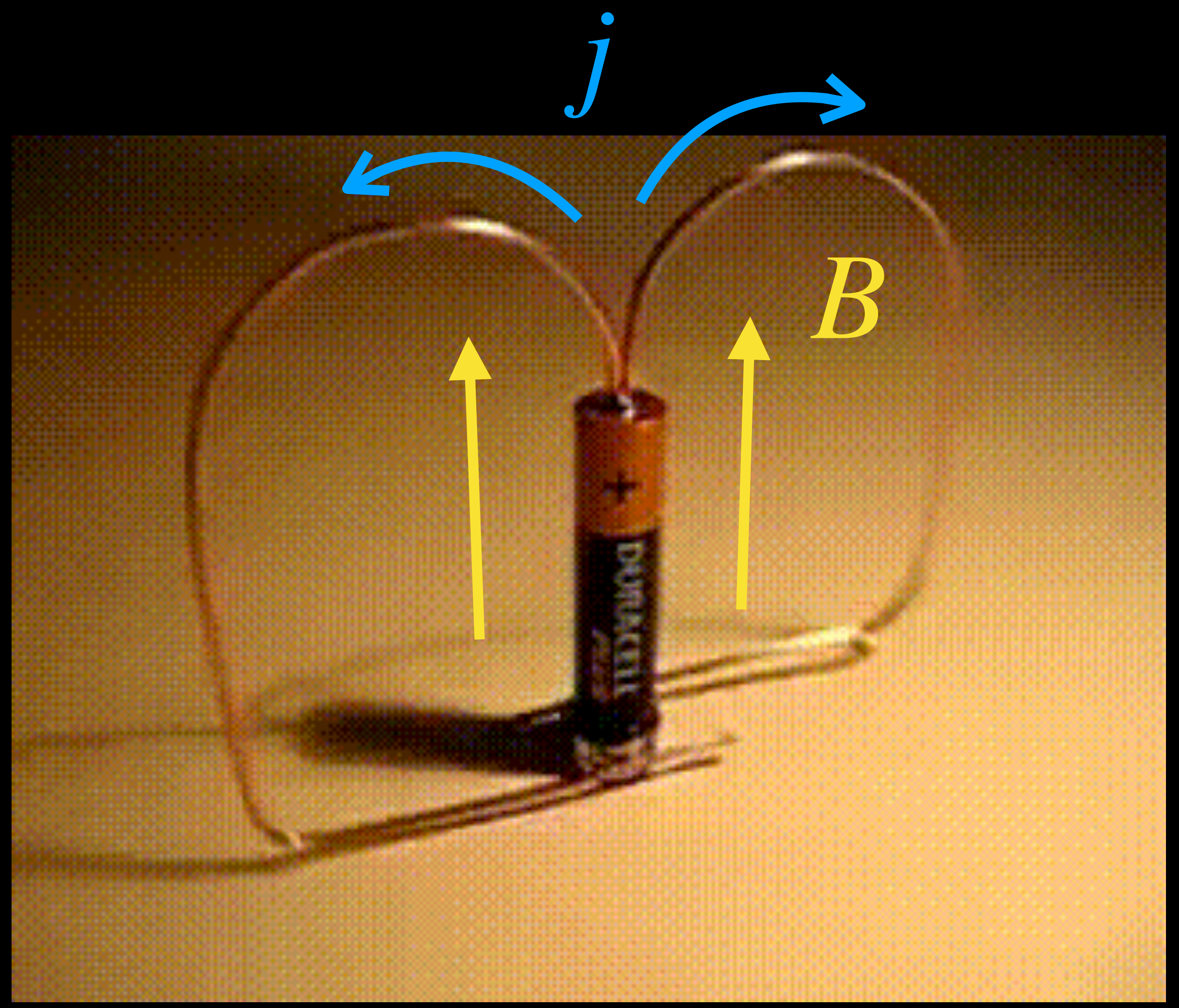

Unipolar induction

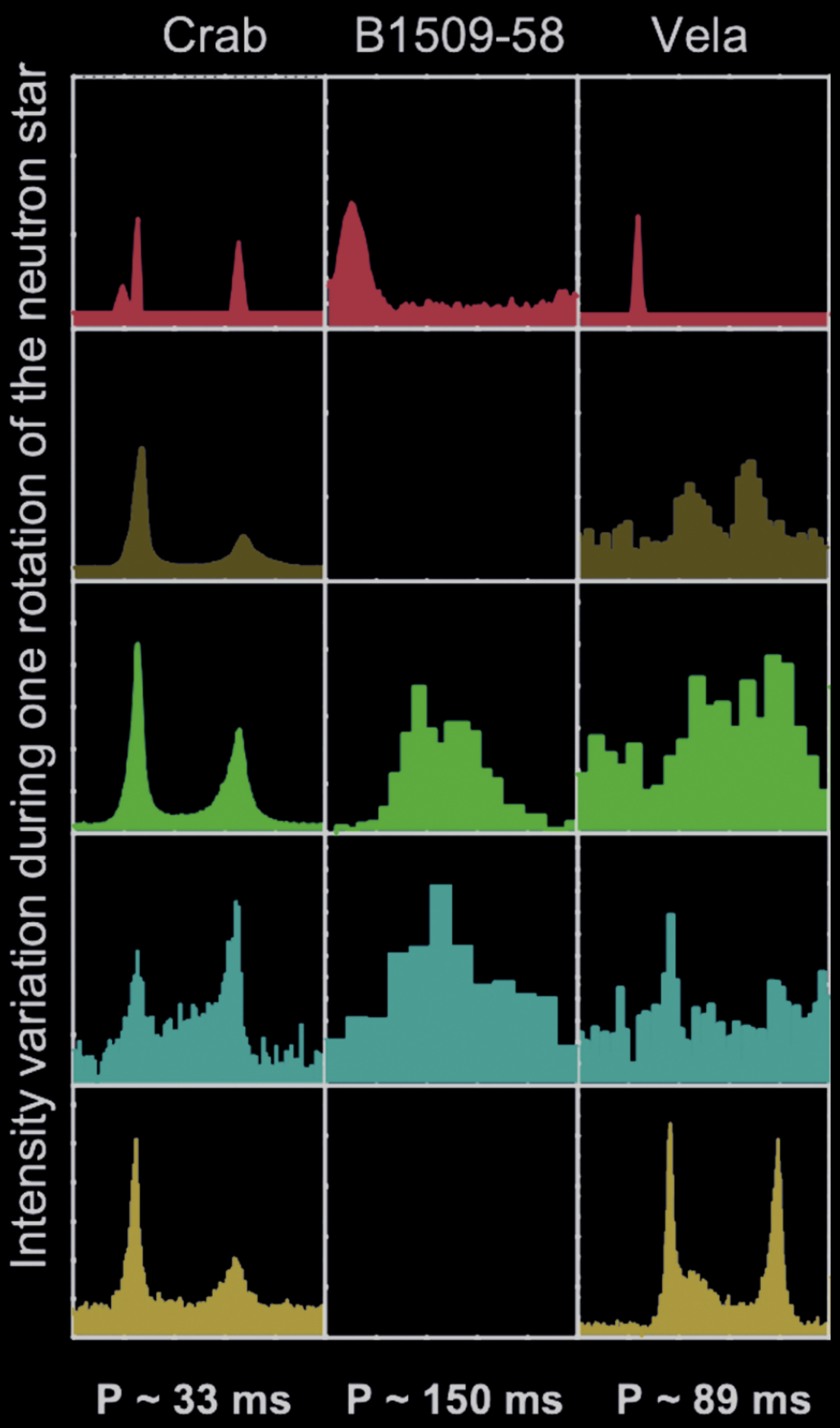

What is a pulsar?

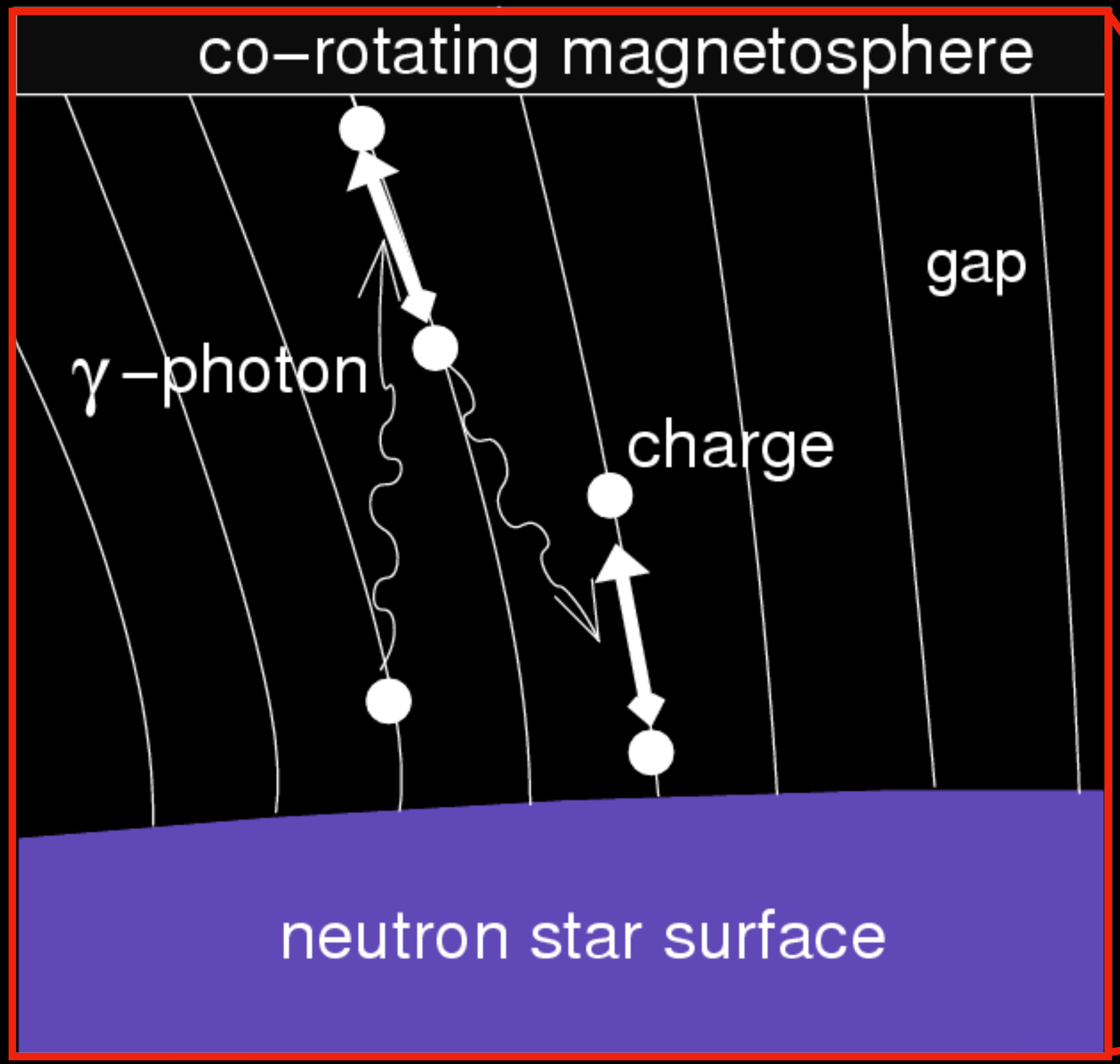

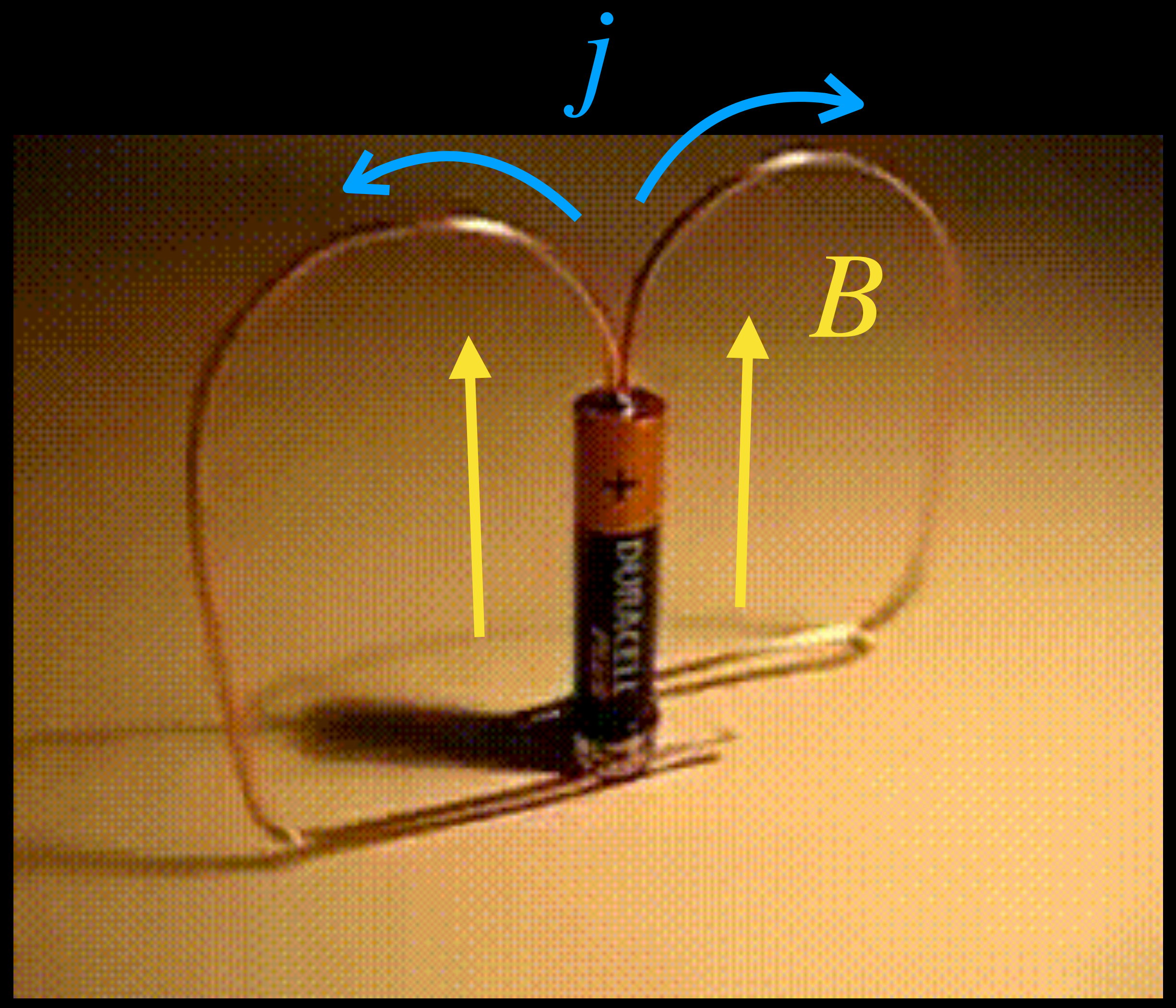

Unipolar induction

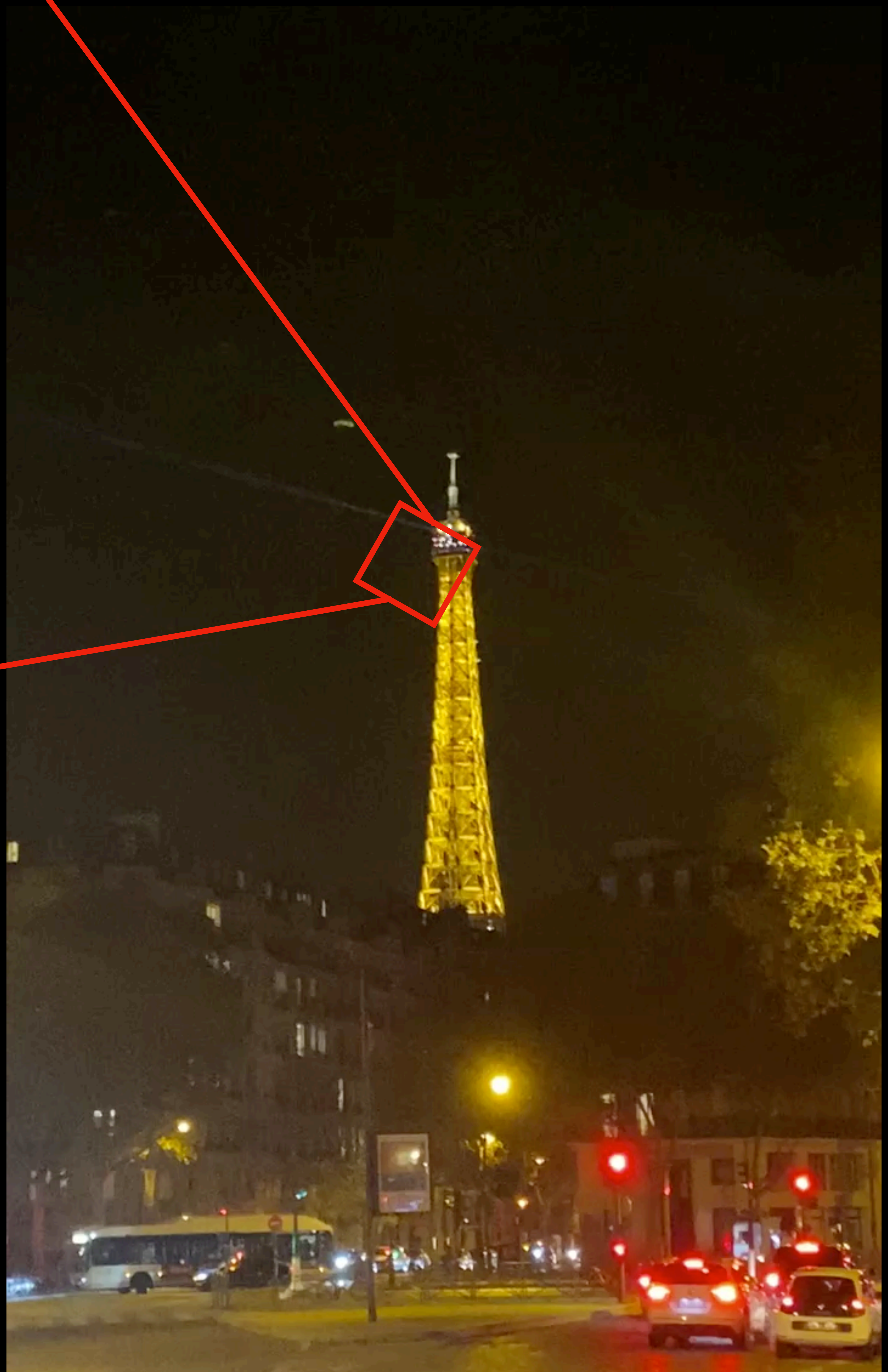

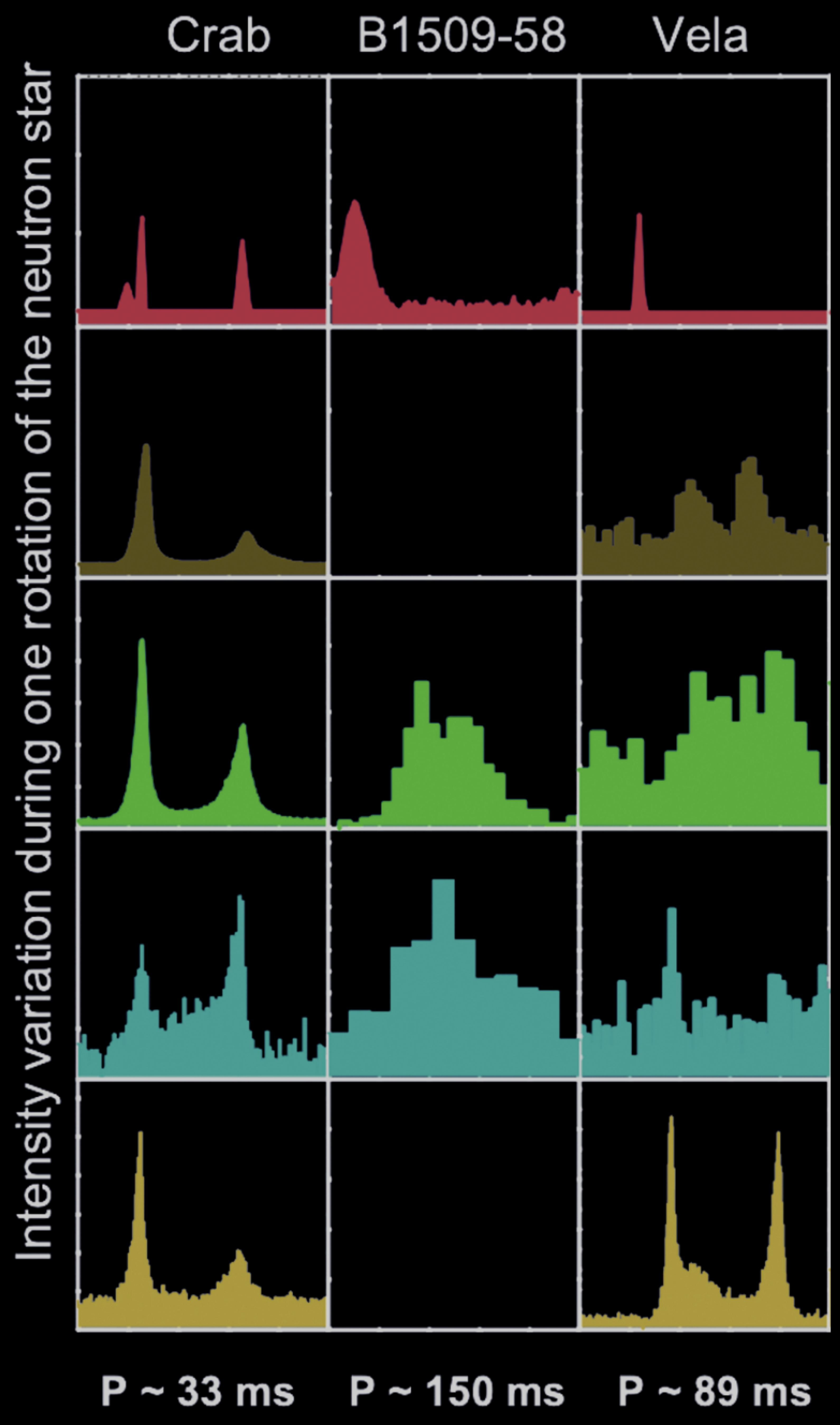

THEORETICAL CARTOON: GJ MODEL

$$\sigma \equiv \frac{B^2/4\pi}{\rho_\pm c^2} \gg 1$$

- Corotation electric field
- Sweepback of $\boldsymbol{B}$-field due to poloidal current
- Poynting flux ⇒ electromagnetic energy losses

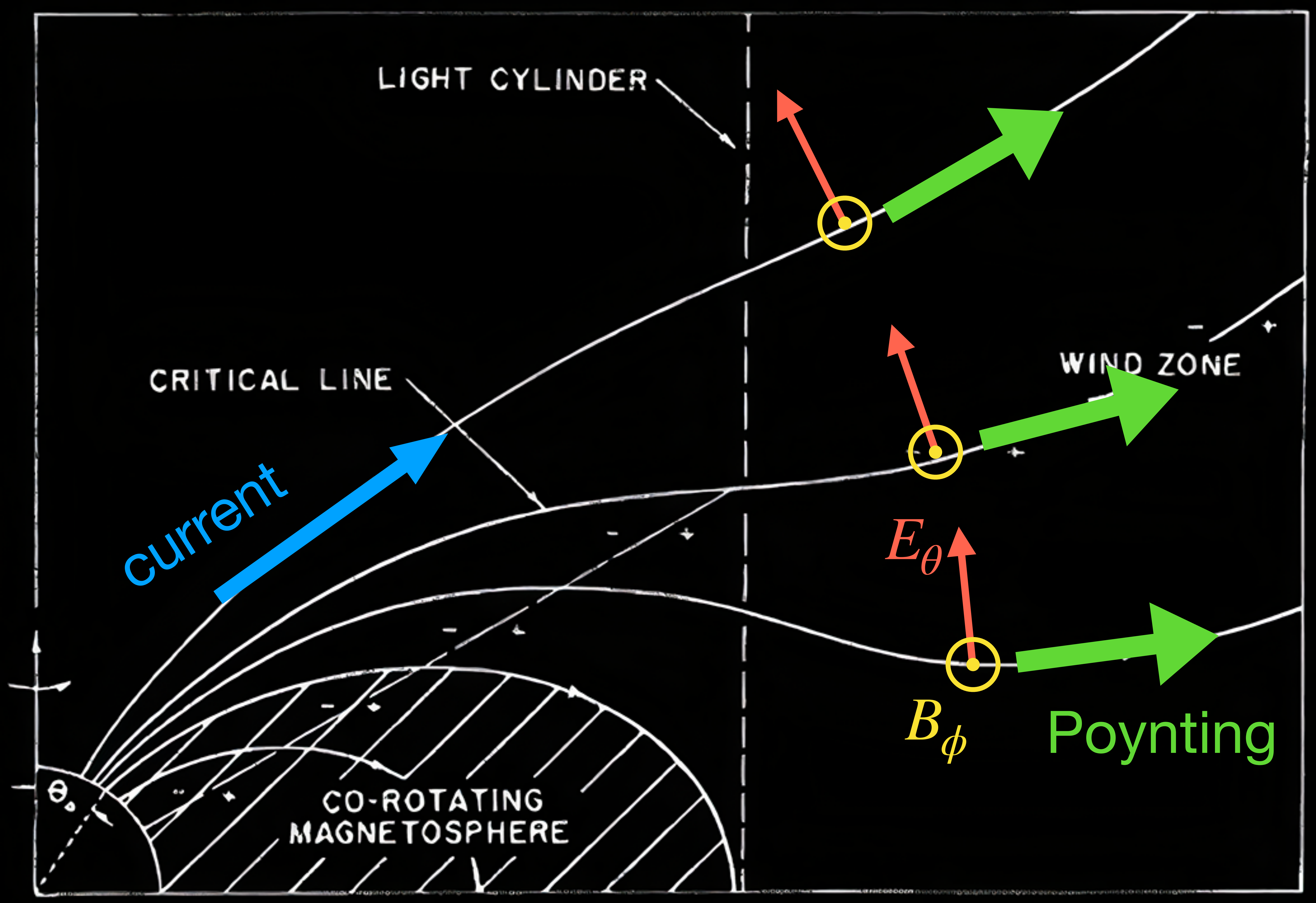

Goldreich & Julian (1969)

THEORETICAL (AND NUMERICAL) APPROACHES

Force-free electrodynamics

Magnetized plasma without inertia

√ OK in highly magnetized regions

- breaks when the existence of plasma is not a given, and in reconnection

• typical apps: neutron star magnetospheres, jets

Magnetohydrodynamics

Plasma as an ideal collisional fluid

√ e.g., no thermal conduction, pressure is same in all directions; OK as a first approximation for global dynamics

- does not describe non-thermal particles

• typical apps: accretion flows

Kinetics

First-principles description for collisionless plasmas

√ includes non-ideal effects (e.g., pressure is different along and across magnetic field, heat flux), describes particle acceleration

- computationally expensive and usually allows limited dynamic range

• typical apps: plasma instabilities, magnetospheres

STANDARD PULSAR

Force-free paradigm

$$\rho_c \boldsymbol{E} + \boldsymbol{j} \times \boldsymbol{B} = \frac{d\rho_m \boldsymbol{u}}{dt} + \text{pressure}, \text{ and } \boldsymbol{E} \cdot \boldsymbol{B} = 0$$

+ Maxwell's equations

$$\Rightarrow \quad \boldsymbol{j} = \boldsymbol{j}(\boldsymbol{E}, \nabla \times \boldsymbol{E}, \nabla \cdot \boldsymbol{E}, \boldsymbol{B}, \nabla \times \boldsymbol{B})$$

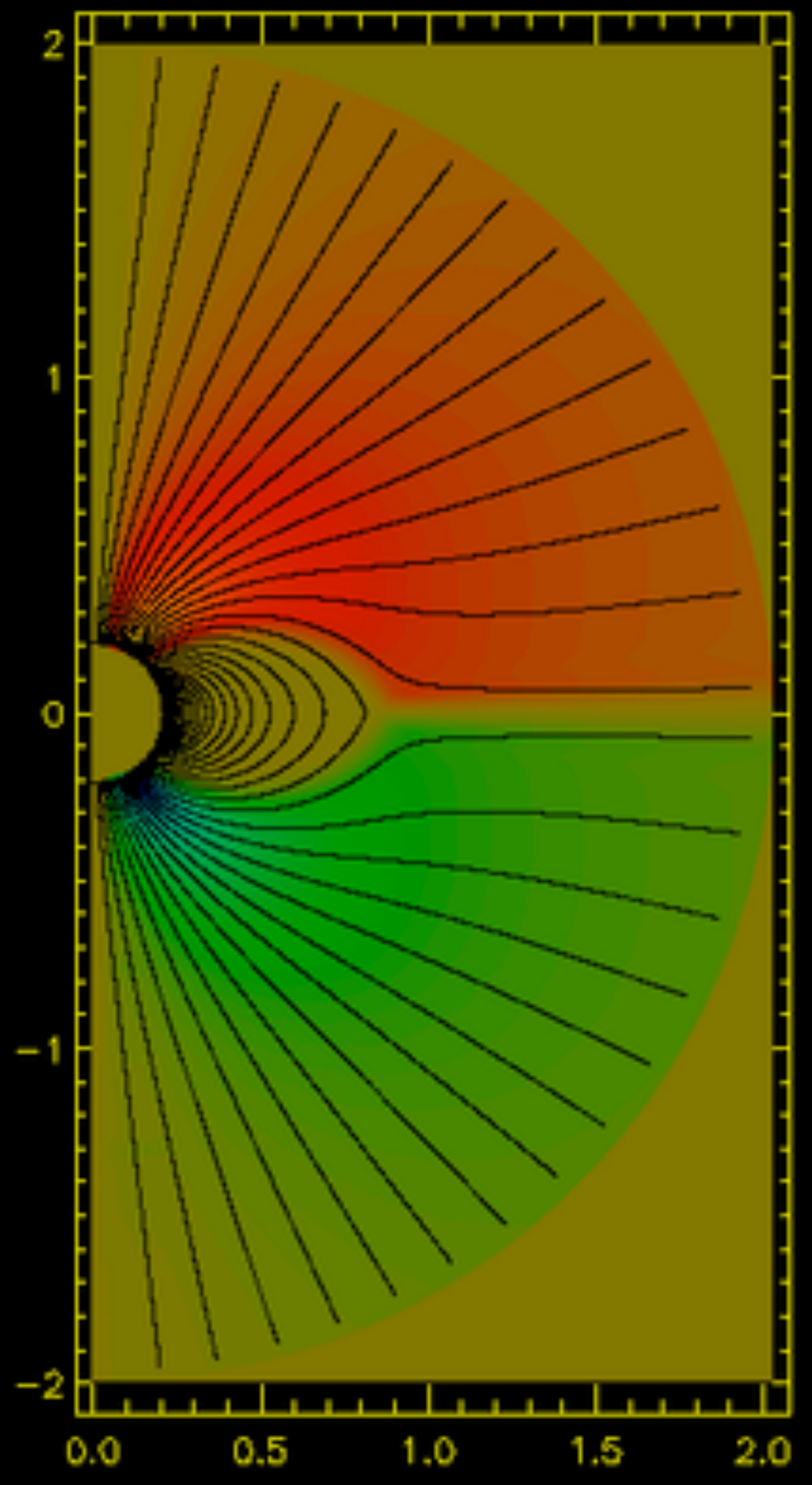

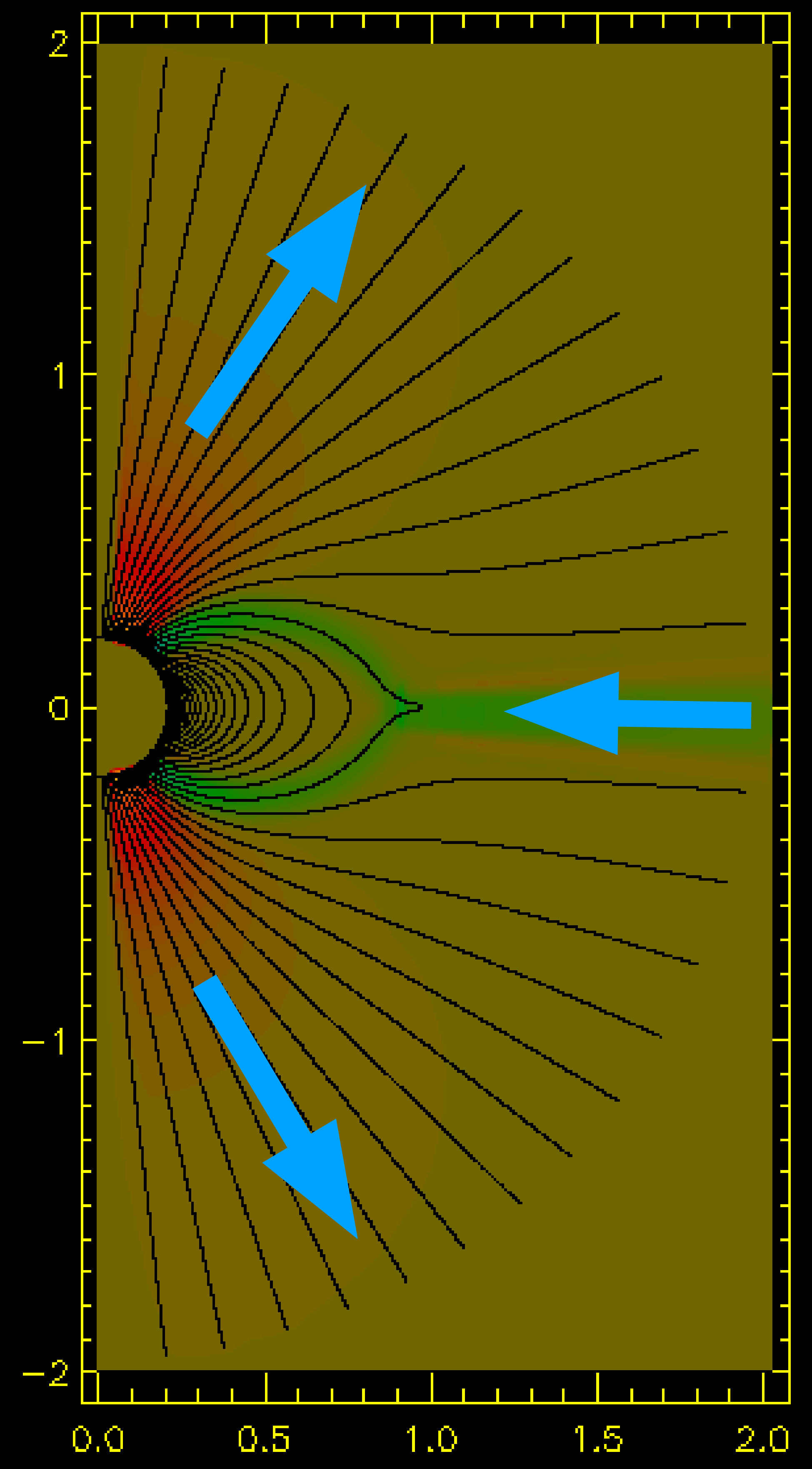

- closed-/open-field-line regions
- equatorial current sheet
- field lines are asymptotically radial
- predicts the spin-down law

$$L_{\rm PSR} = k_1 \frac{\mu^2 \Omega^4}{c^3} \left(1 + k_2 \sin^2 \alpha\right)$$

- can not predict: particle acceleration, plasma supply, non-thermal radiation

Contopoulos+ (1999), Spitkovsky (2006), Kalapotharakos (2009), Petri (2012), Tchekhovskoy+ (2014) (MHD)

Plasma Physics on a computer: (GR)(R)PIC

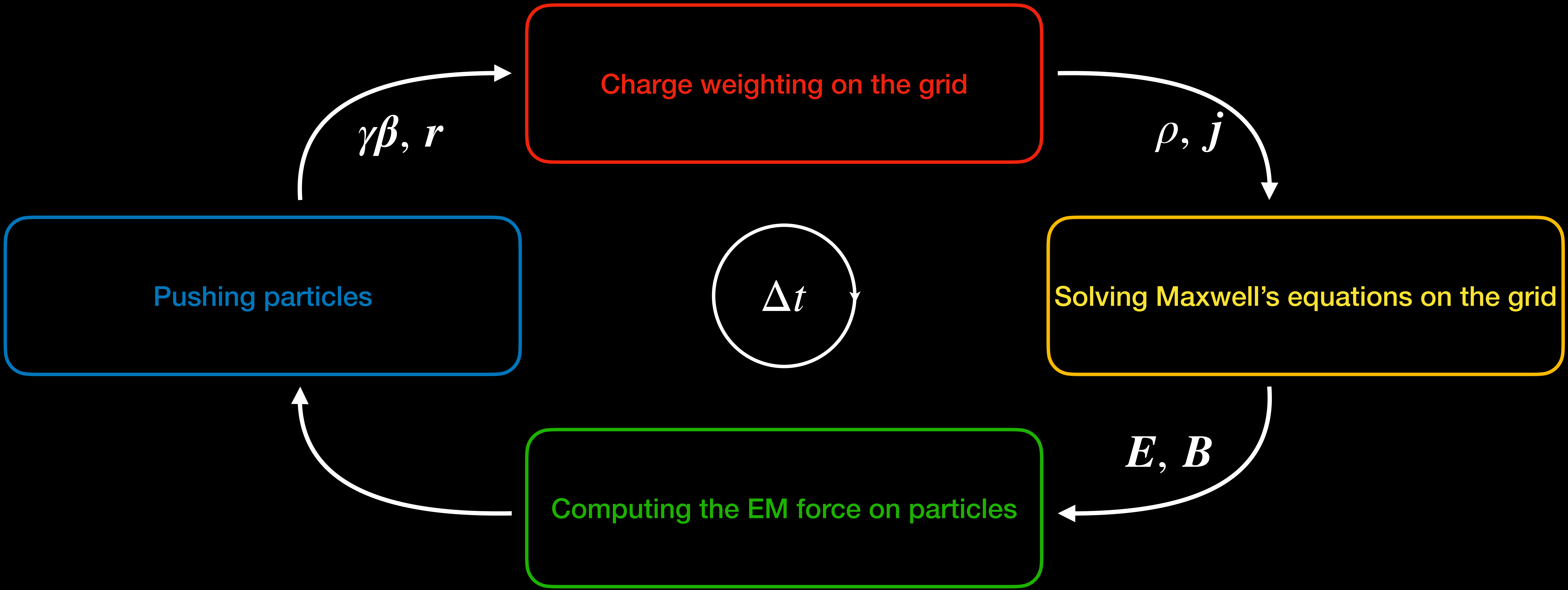

(GR) = general relativistic

(R) = radiation reaction force, photon emission, multiple pair production mechanisms

PIC = particle-in-cell

Magnetospheric Structure and High-Energy Emission

(GR) OBLIQUE ROTATOR WITH PAIR PRODUCTION

Philippov, Spitkovsky, 2018 (ApJ)

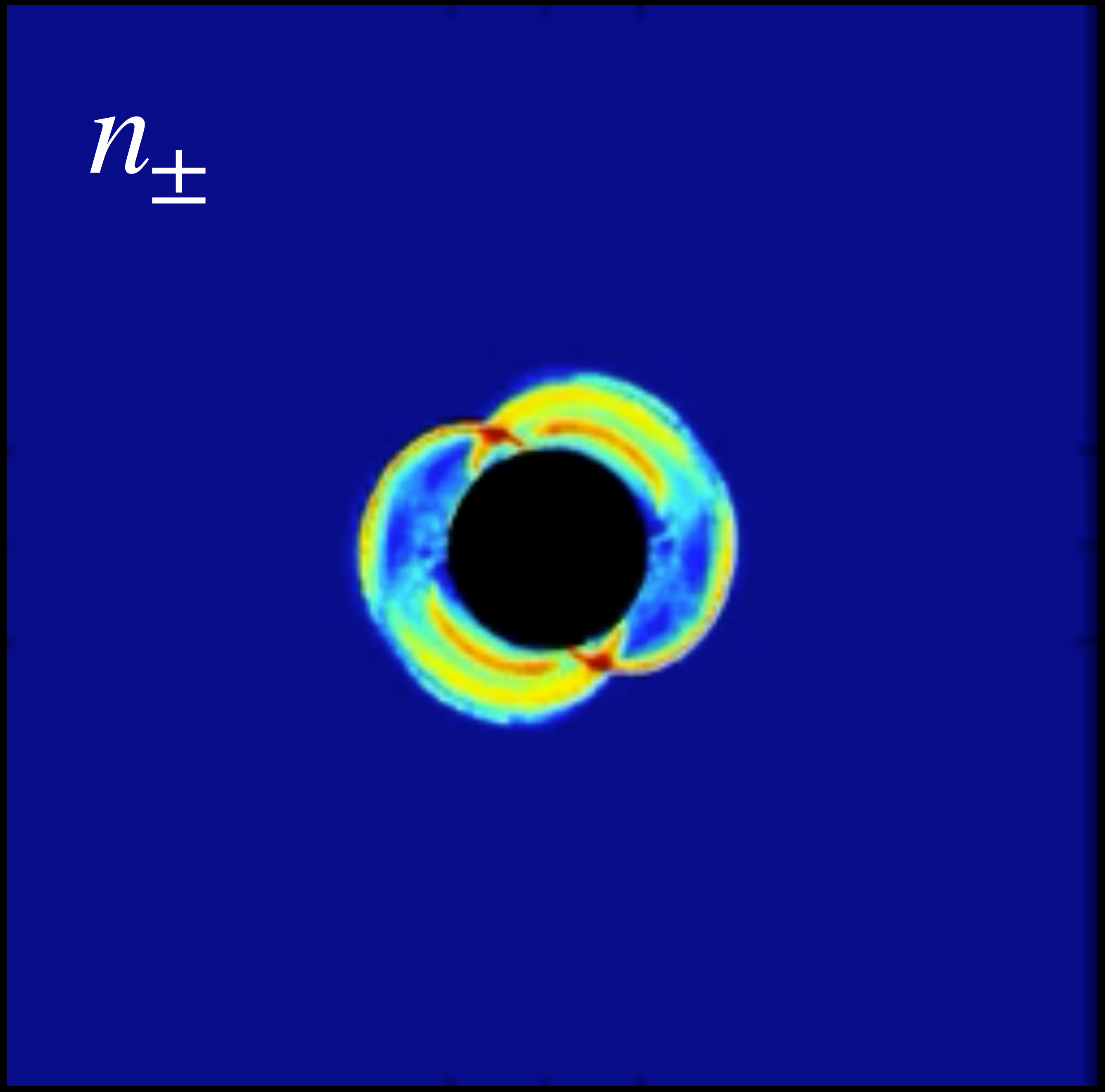

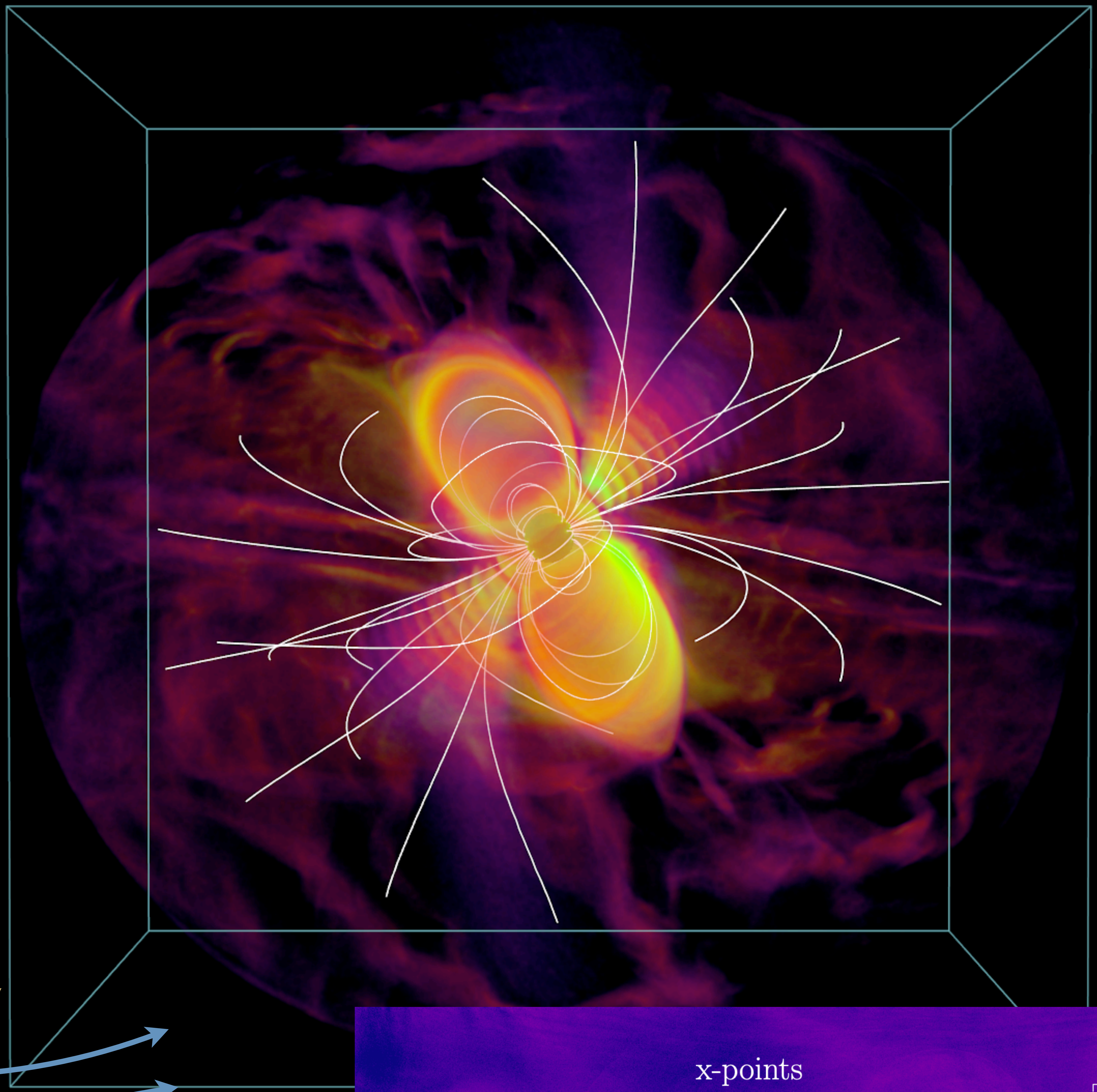

- Non-stationary discharge powers coherent radio emission.
- Relativistic magnetic reconnection in the current sheet powers high-energy emission. Its rate controls the radiated power.
- Current sheet is unstable to plasmoid (tearing) and drift-kink instabilities.

Hakobyan, Philippov et al., 2019 (ApJ)

(and many others after Loureiro et al., 2007)

2D:

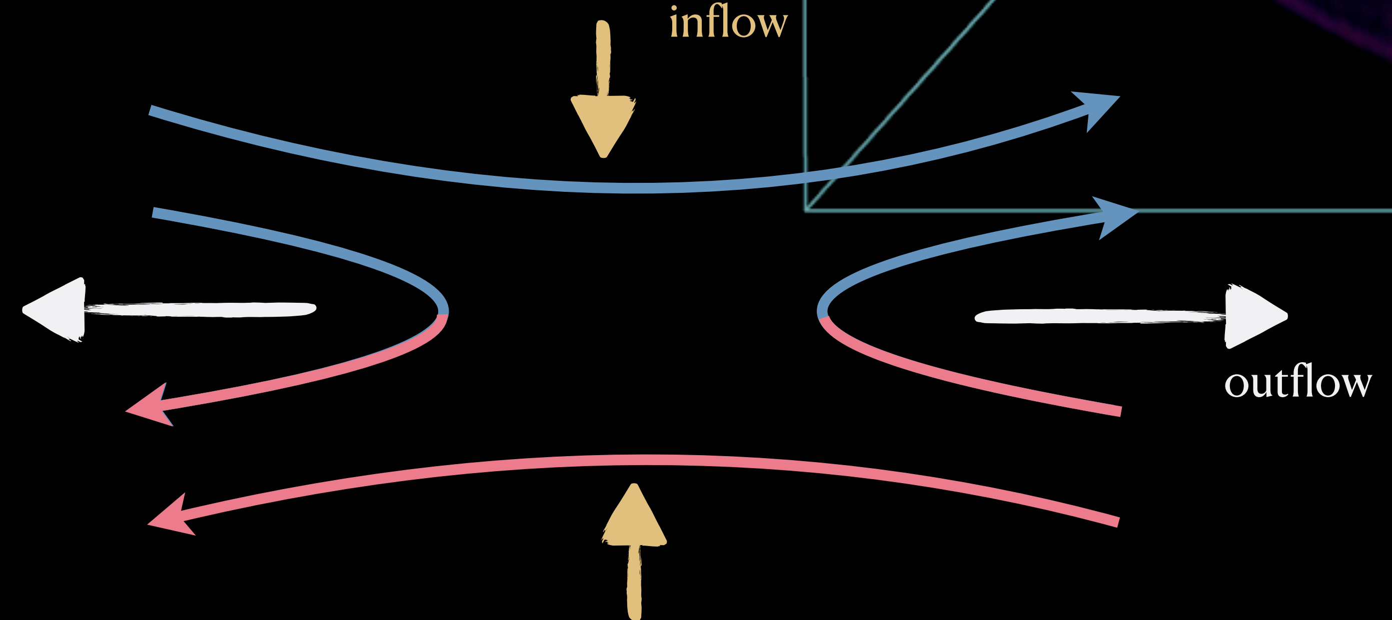

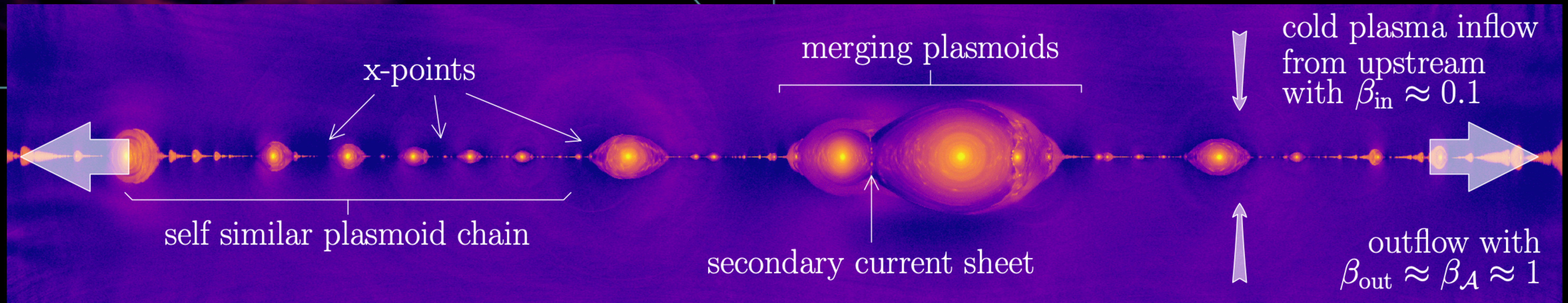

Gamma-ray emission modeling

- Simulations prefer current sheet as a particle accelerator
- Particles radiate synchrotron emission
- Observe caustic emission
- Predict gamma-ray efficiencies 1-20% depending on the inclination angle and pair production efficiency in the sheet
- Higher inclinations are less dissipative

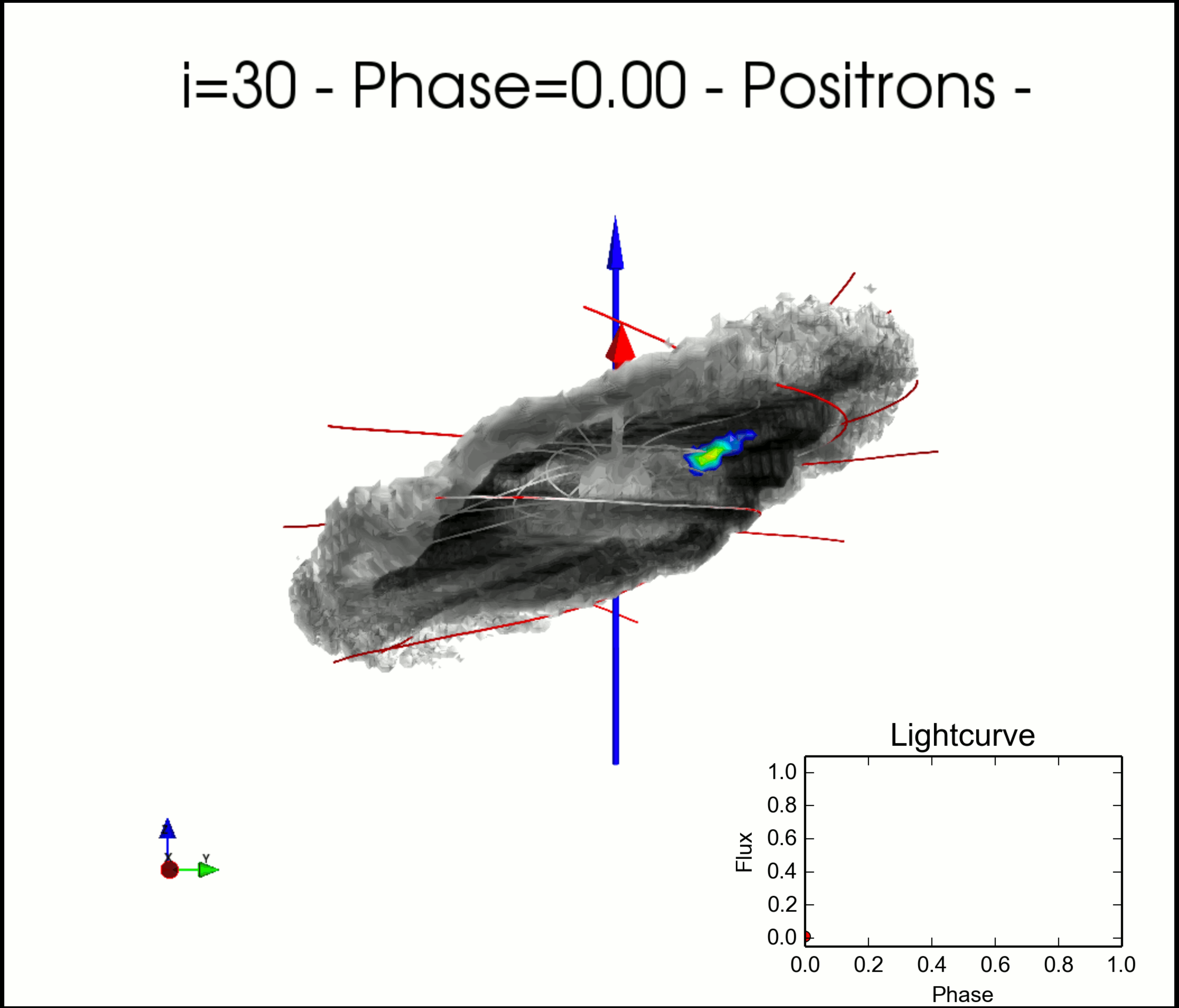

Cerutti, Philippov, Spitkovsky, 2016 (MNRAS); Philippov, Spitkovsky, 2018 (ApJ)

LIGHTCURVES

FERMI

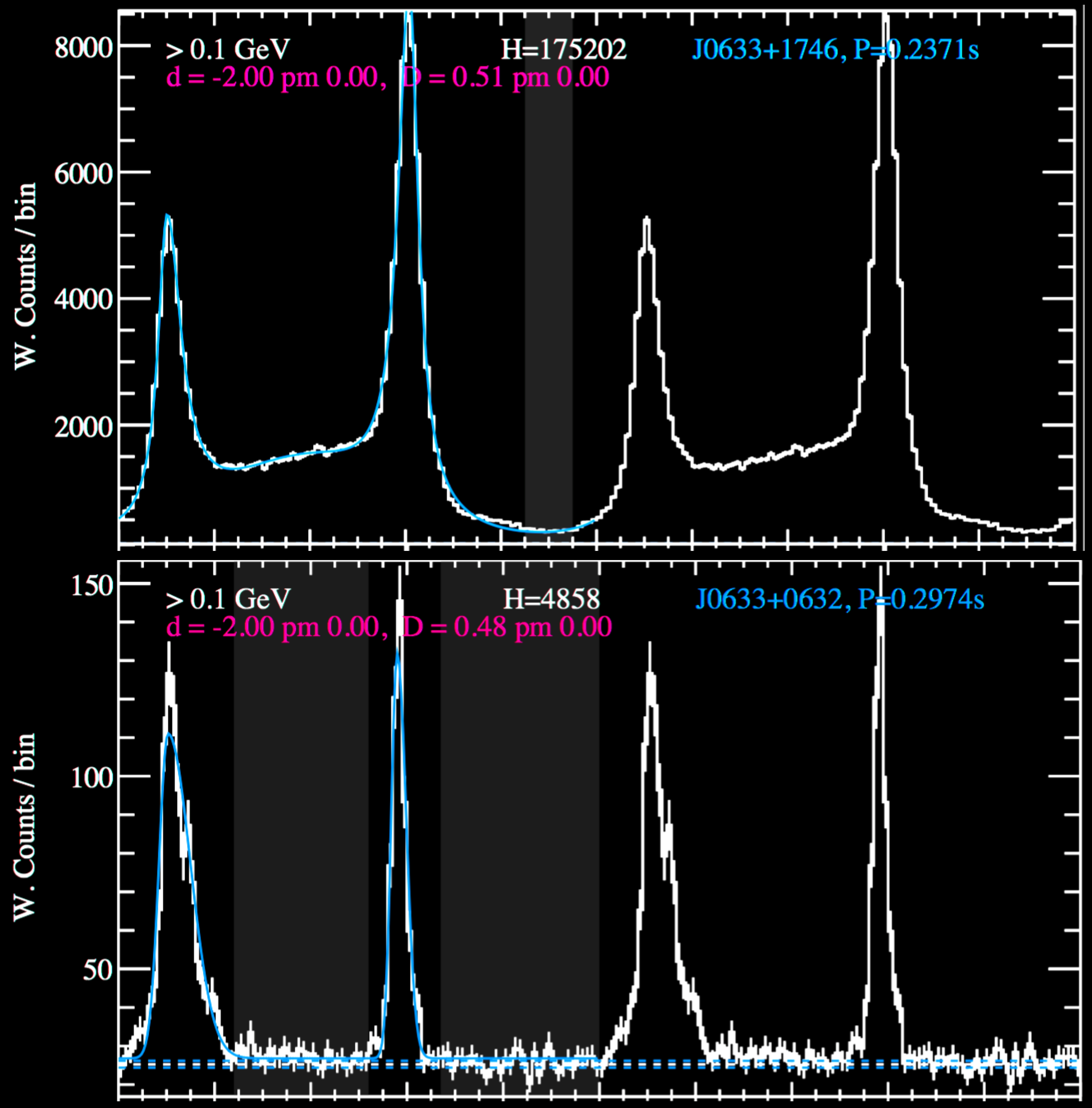

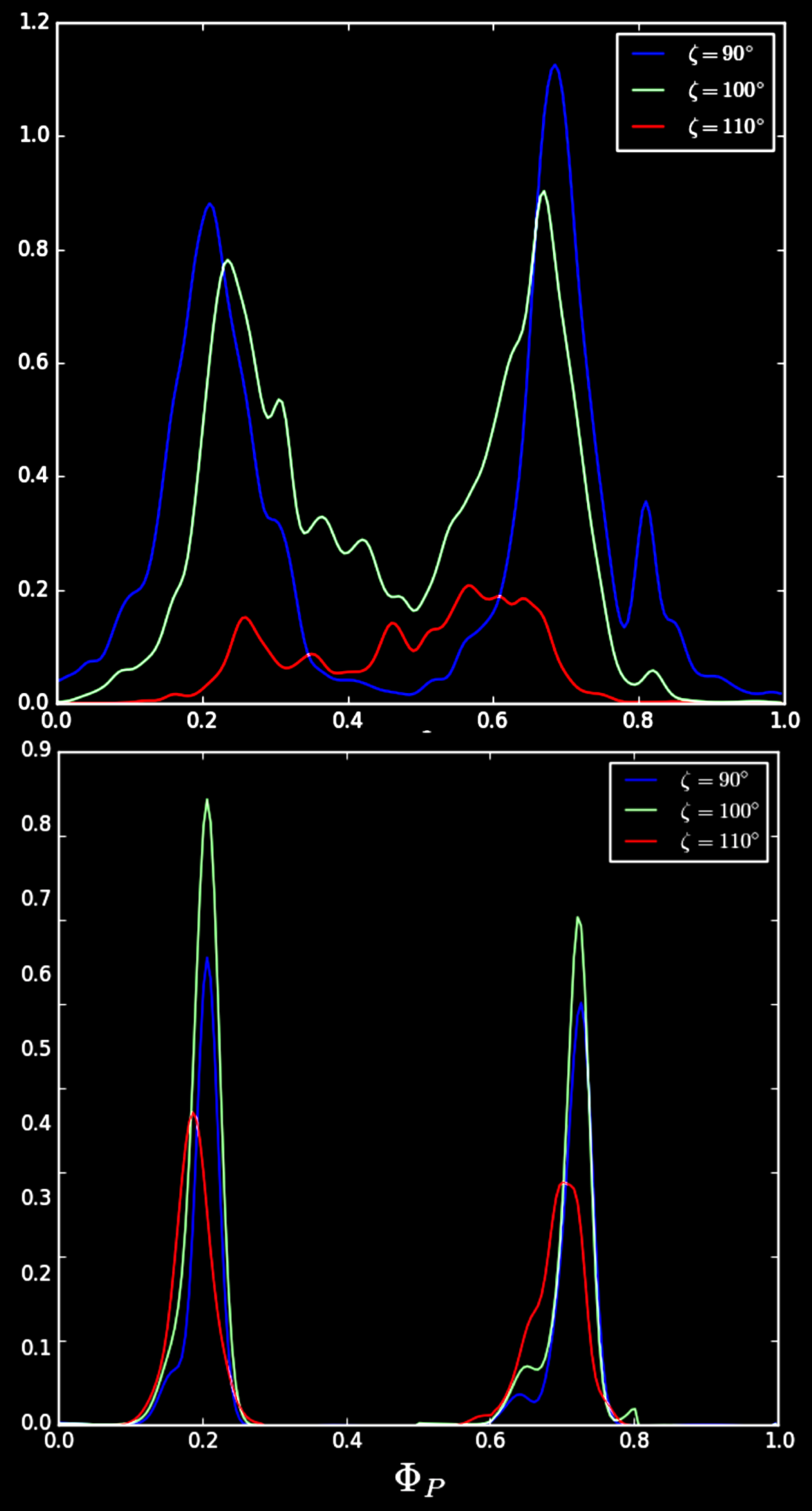

Double-peaked lightcurves are generic

Philippov, Spitkovsky, 2018 (ApJ)

Reconnection in pulsar magnetospheres

- $B \sim 10^5$ G, $\sigma = B^2/(4\pi\rho_m c^2) \gg 1$
- Reconnection electric field accelerates particles, synchrotron cooling is important on the same timescale
- Pairs accelerate beyond the radiation reaction limit, up to $\gamma \sim \text{few} \times \sigma$
- Highest energy photons are beamed along the upstream magnetic field, consistent with the beaming of GeV lightcurves

$$h\nu_{\max} \approx 16 \text{ MeV} \cdot \left(\sigma/\gamma_{\text{syn}}\right)$$

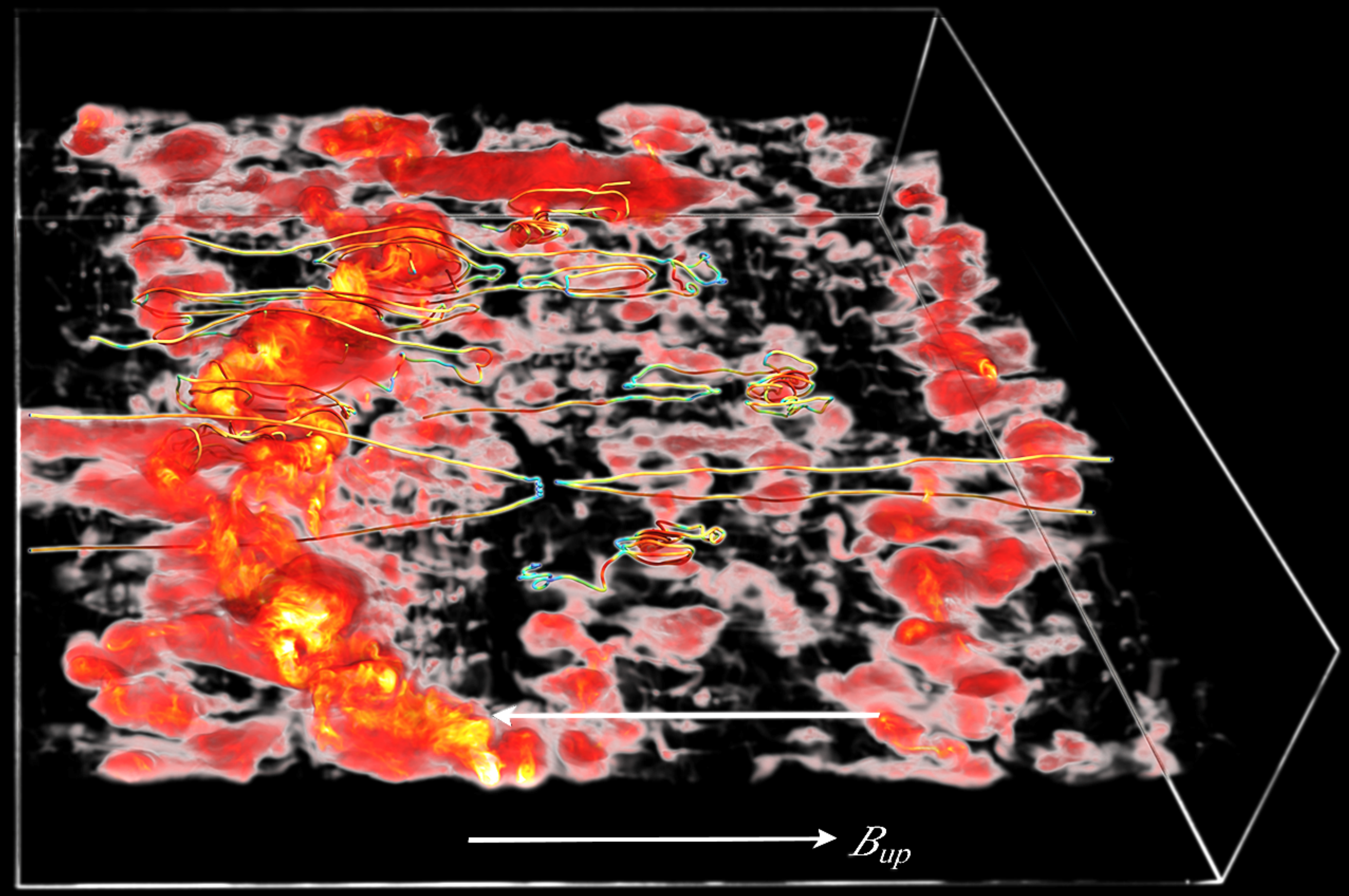

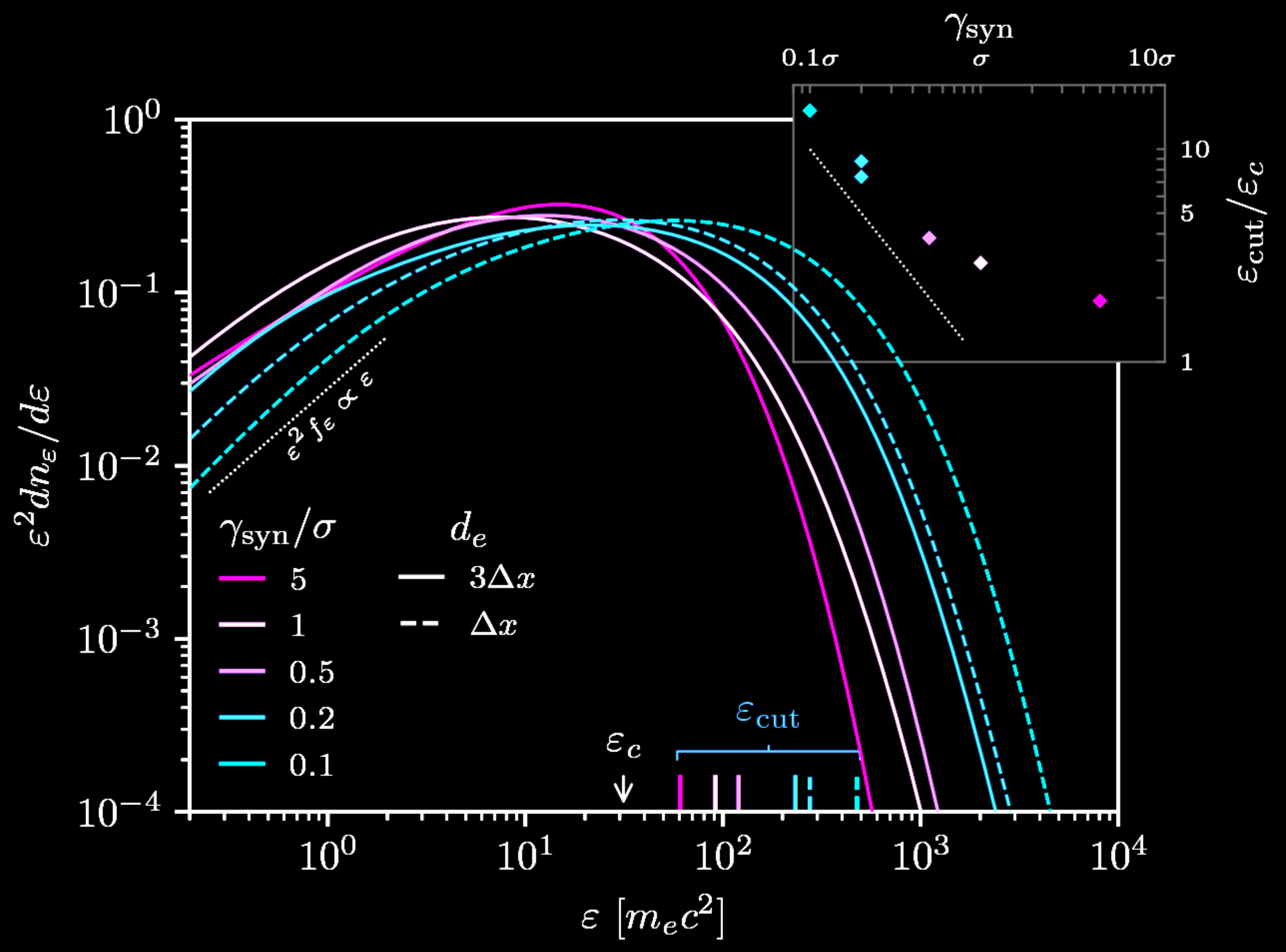

Chernoglazov, Hakobyan, Philippov, 2023 (ApJ)

New frontier: multi-TeV from Vela pulsar [in prep]

The H.E.S.S. Collaboration, Nature (2023)

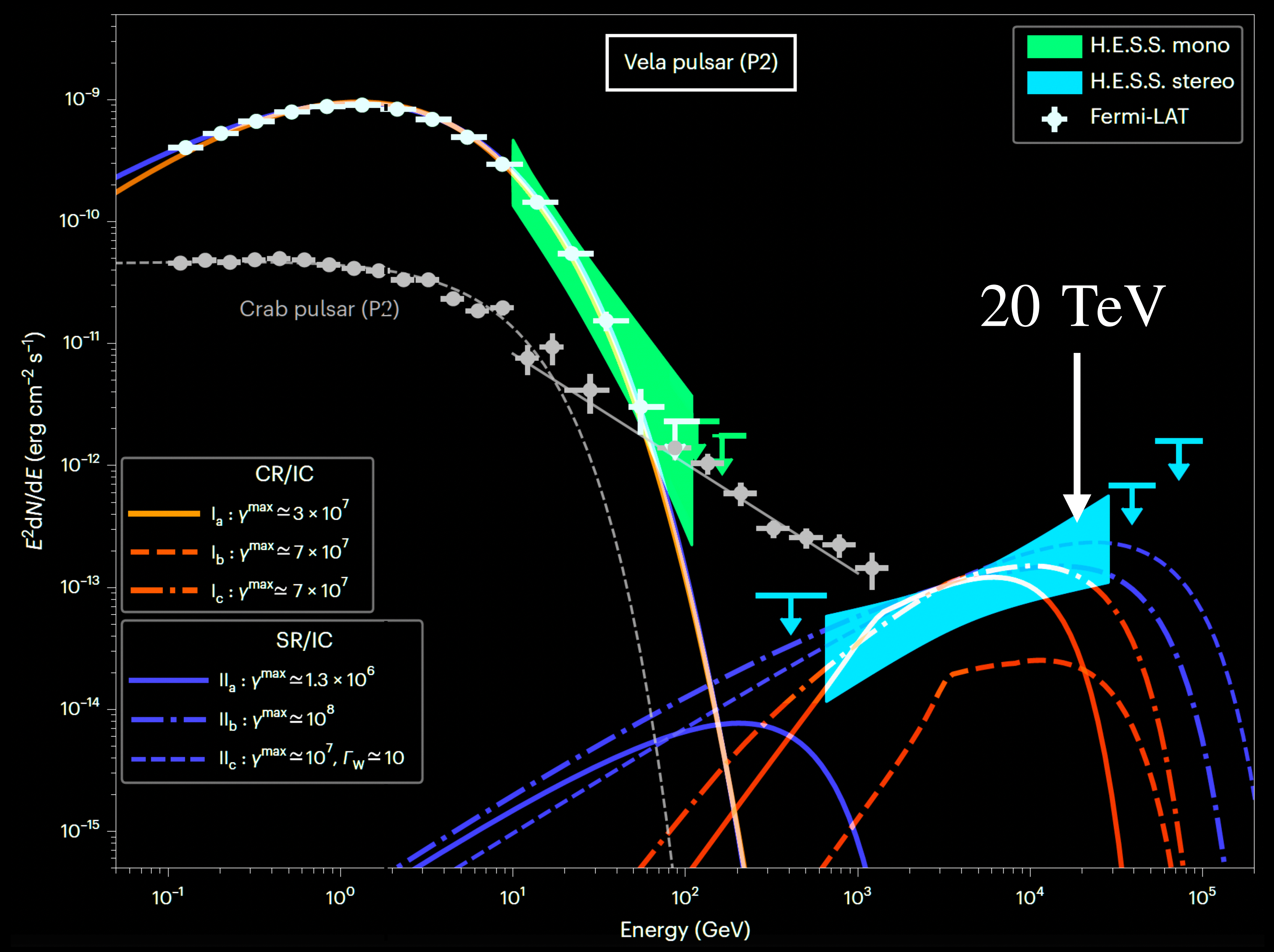

Bransgrove et al, 2023 (ApJL)

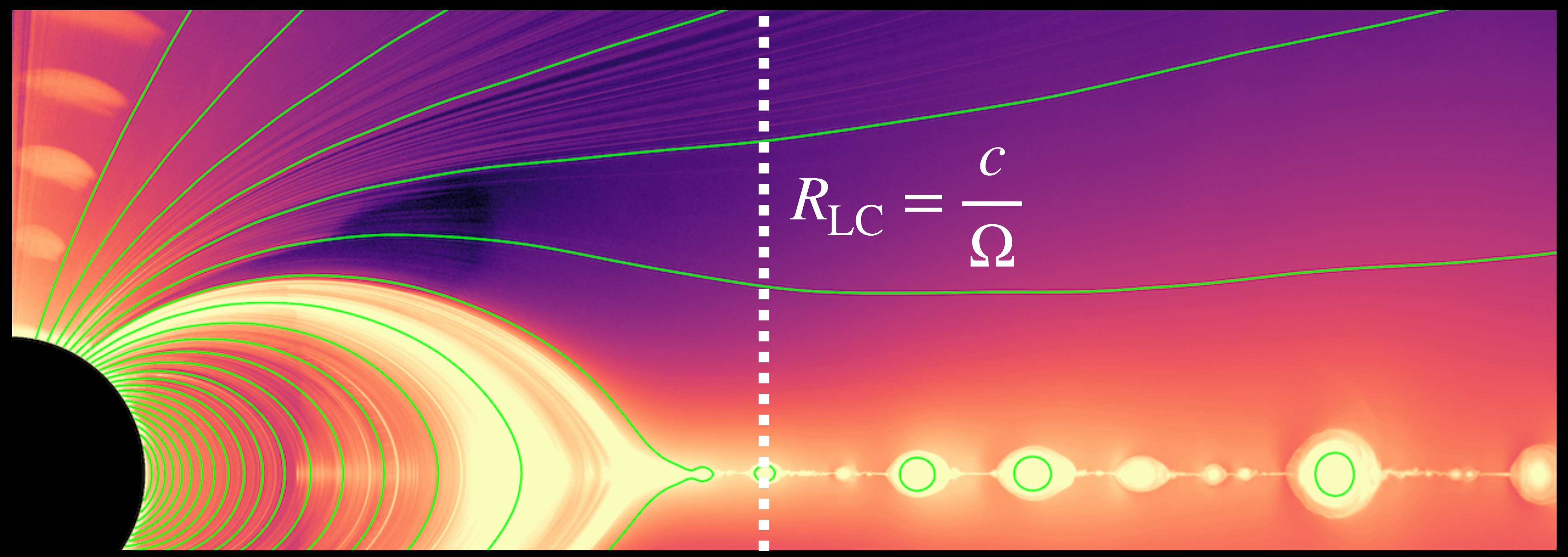

$$\gamma_{syn} \approx 10^5 \quad \Rightarrow \quad \sigma \approx \text{few} \times 10^7$$

$$\uparrow$$

$$\varepsilon_{ph} = 16 \text{ MeV} \cdot \left(\sigma / \gamma_{syn}\right)$$

$$m_e c^2 \gamma_{max} = m_e c^2 \sigma \sim 10 \text{ TeV}$$

- Pair density is low because "return"-current discharge sends most of the plasma into the star
- Most of the plasma is produced in the current sheet

Prediction: CTA will see moderately energetic γ-ray pulsars as multi-TeV sources

New frontier: multi-TeV from Vela pulsar [in prep]

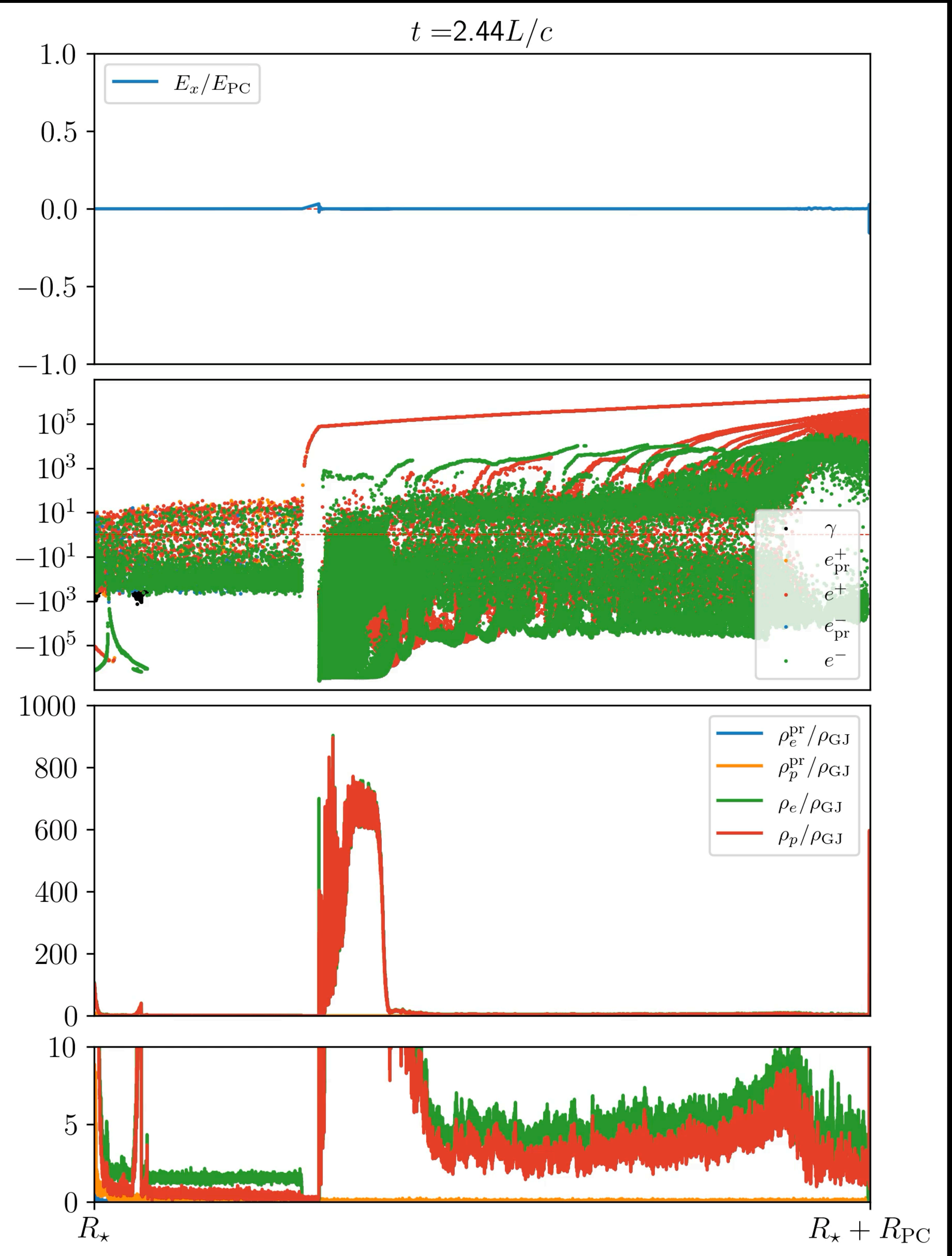

$$\gamma_{syn} \approx 10^5 \quad \Rightarrow \quad \sigma \approx \text{few} \times 10^7$$

$$\uparrow$$

$$\varepsilon_{ph} = 16 \text{ MeV} \cdot \left(\sigma/\gamma_{syn}\right)$$

$$m_e c^2 \gamma_{max} = m_e c^2 \sigma \sim 10 \text{ TeV}$$

- Pair density is low because "return"-current discharge sends most of the plasma into the star
- Most of the plasma is produced in the current sheet

Prediction: CTA will see moderately energetic γ-ray pulsars as multi-TeV sources

Radio Emission

POLAR RADIO EMISSION

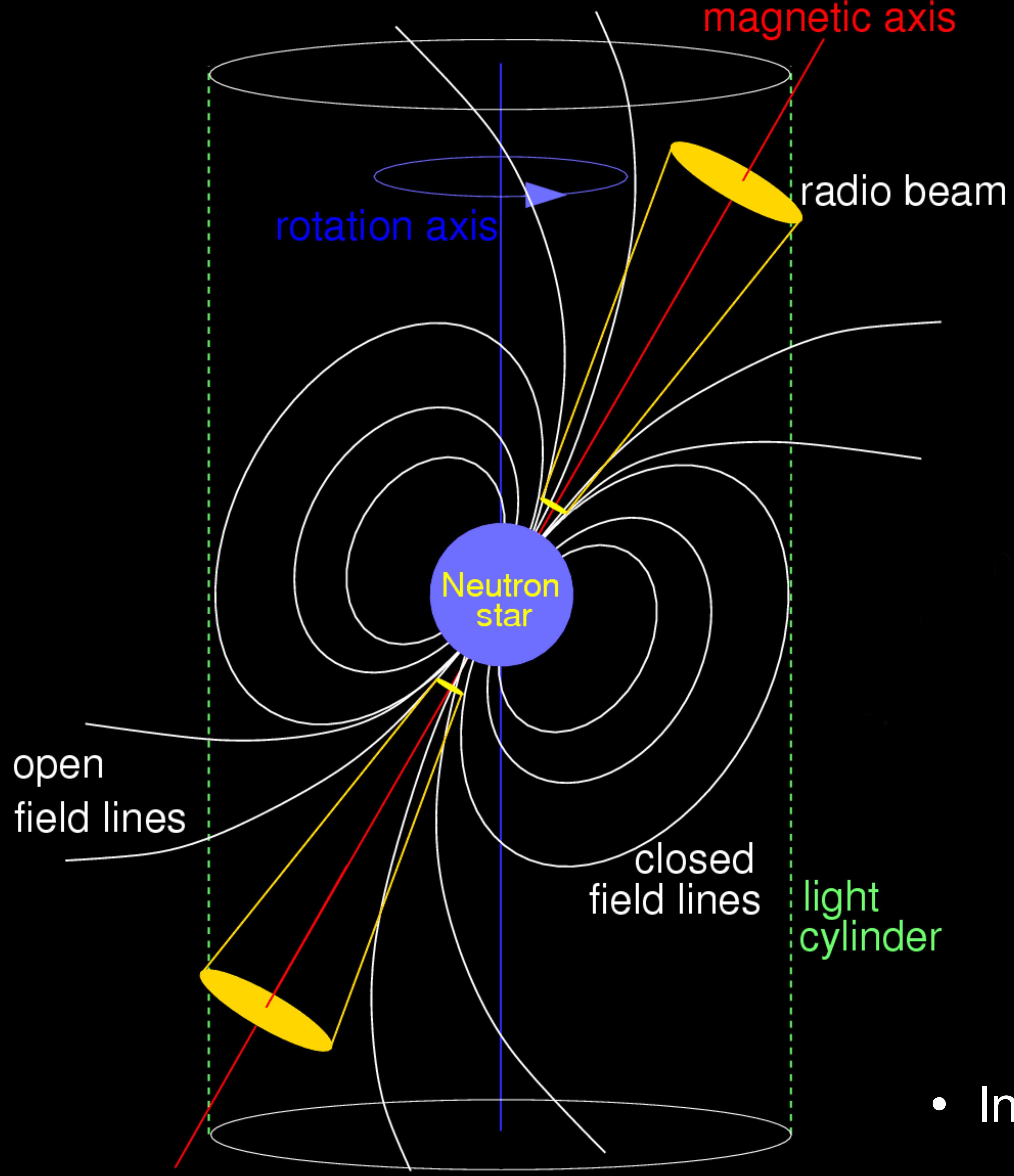

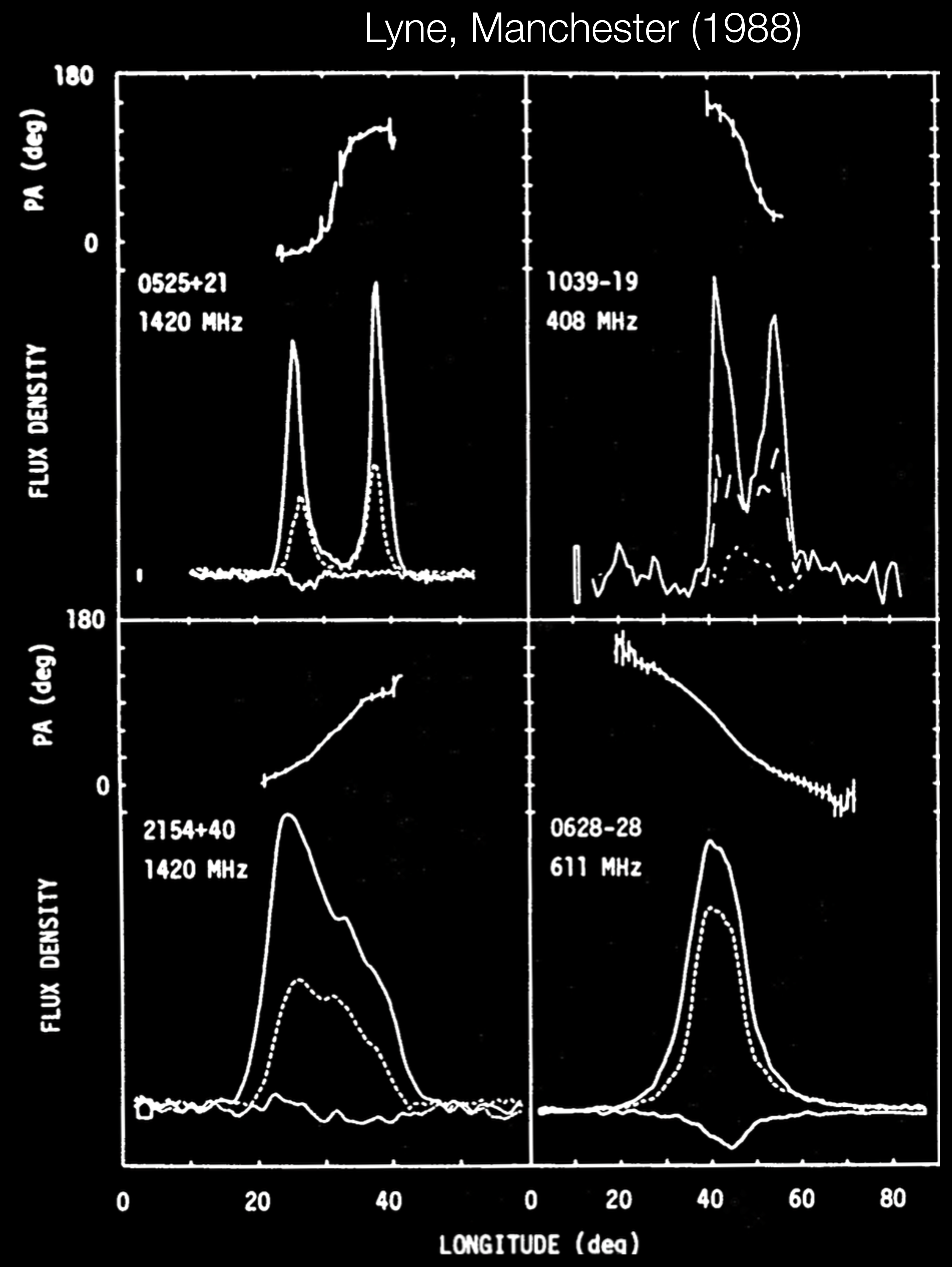

- In most cases we see one short pulse per period
- Beam width is related to the polar cap size

Hints from Global Simulations

- Non-stationary discharge drives waves in the polar region.
- Waves are generated during the process of electric field screening. They are driven by collective plasma motions, thus, coherent *(see also Beloborodov 2008; Timokhin, Arons 2013)*.

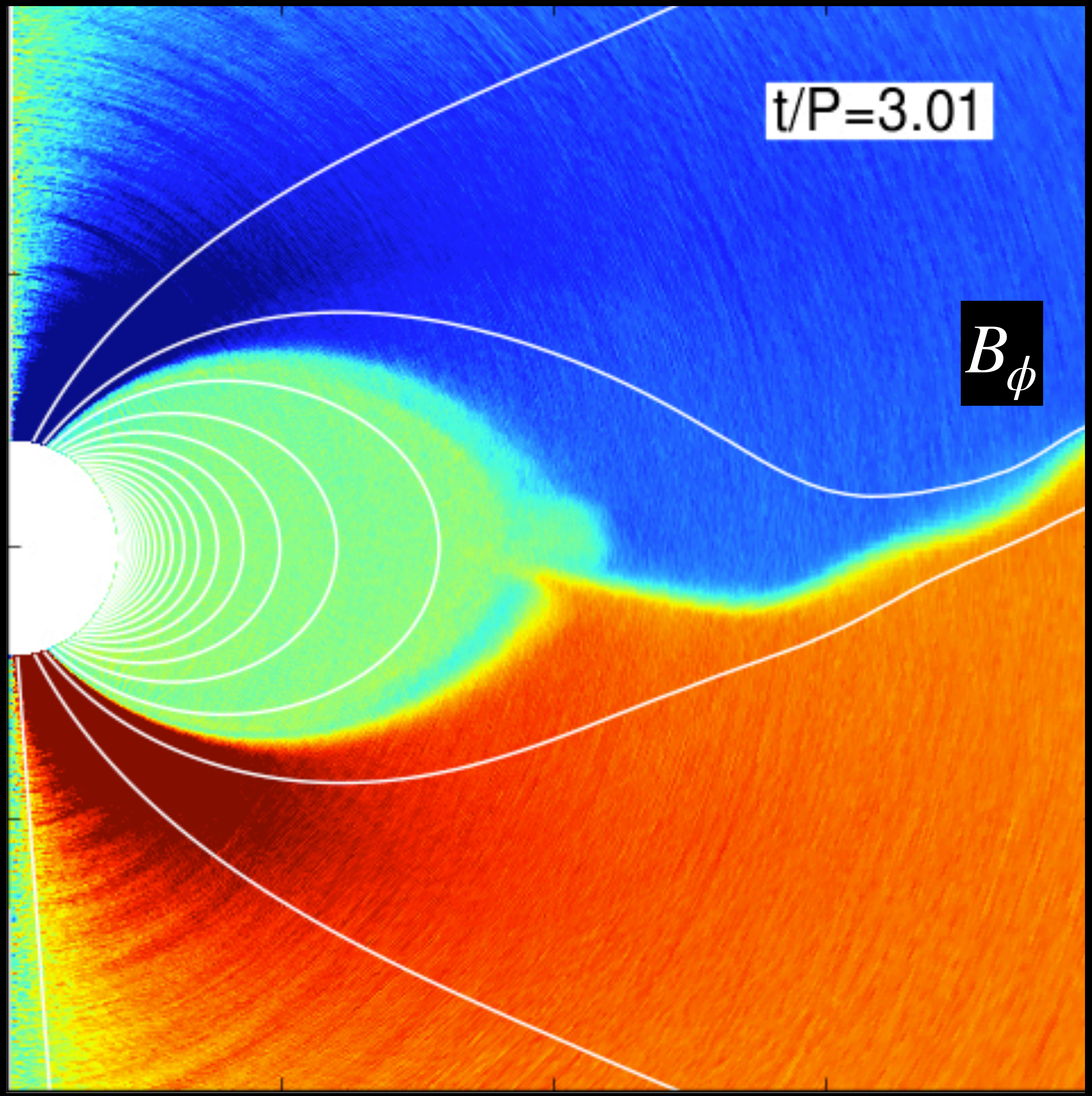

Philippov et. al. (2015)

Local simulation of 2D discharge

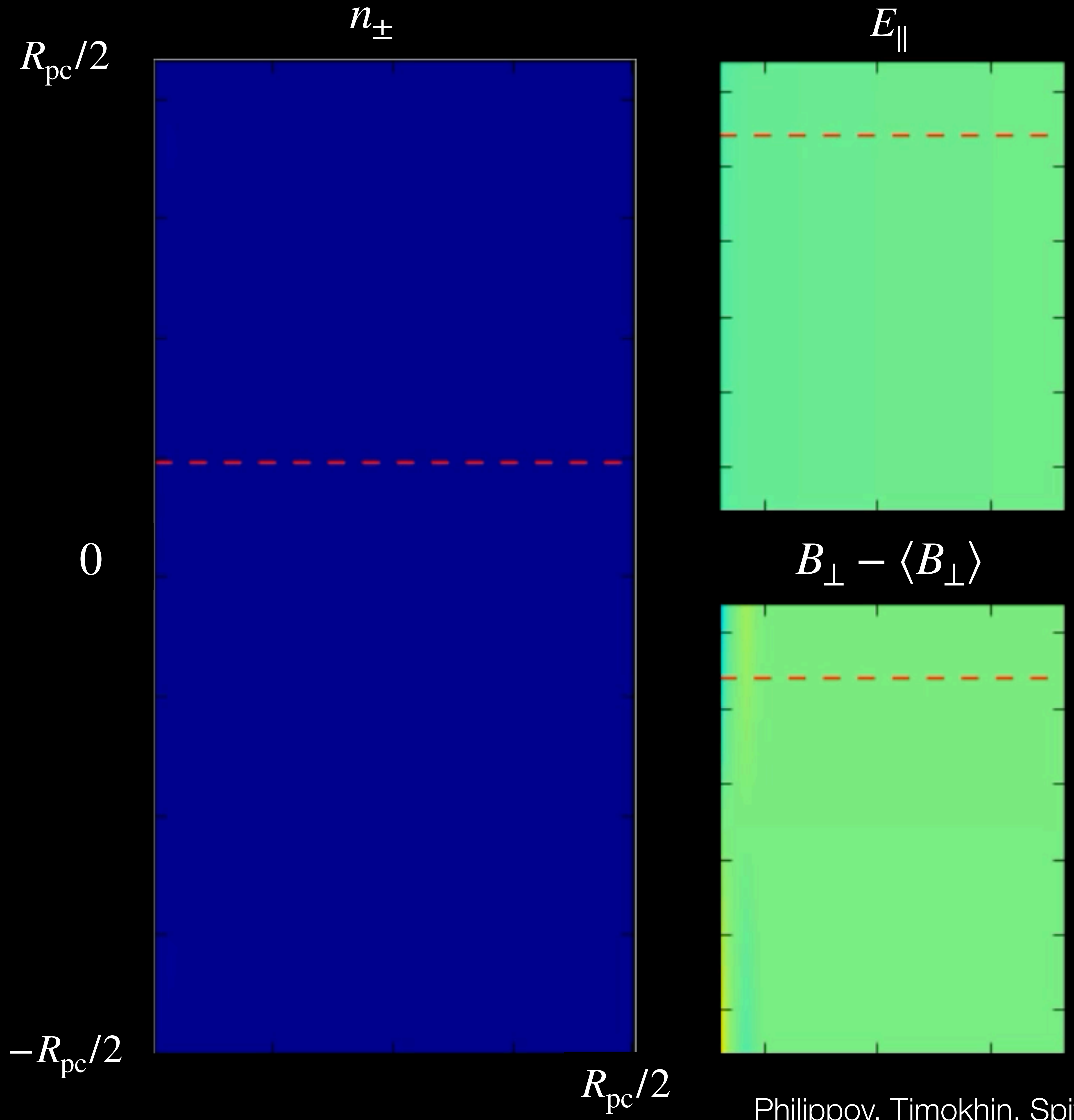

- Intermittency of the discharge results in production of coherent currents that are "screening" the electric field
- Oblique "screening" waves are electromagnetic and superluminal; thus, can escape from the magnetosphere
- The power if fixed at $\sim 10^{-4} L_{sd}$

Philippov, Timokhin, Spitkovsky, 2020 (PRL)

See also Cruz et. al., 2021, Bransgrove et. al., 2023 (ApJL)

SPECTRUM OF A 1D DISCHARGE

- Power cascades to a maximum plasma frequency in the cloud
- Clearly a very broad-band mechanism

$$\nu \simeq \sqrt{4\pi e^2 \kappa n_{\rm GJ}/\langle\gamma^3\rangle m_e^3}/2\pi \sim 26\sqrt{\kappa_5 B_{12}/r^3 P_{0.1}\gamma_{10}^3}\ \text{GHz}$$

Prediction: close-by young pulsars should be ALMA sources

Tolman, Philippov, Timokhin, 2022 (ApJL)

CONFIRMATION WITH DIFFERENT NUMERICAL CODES

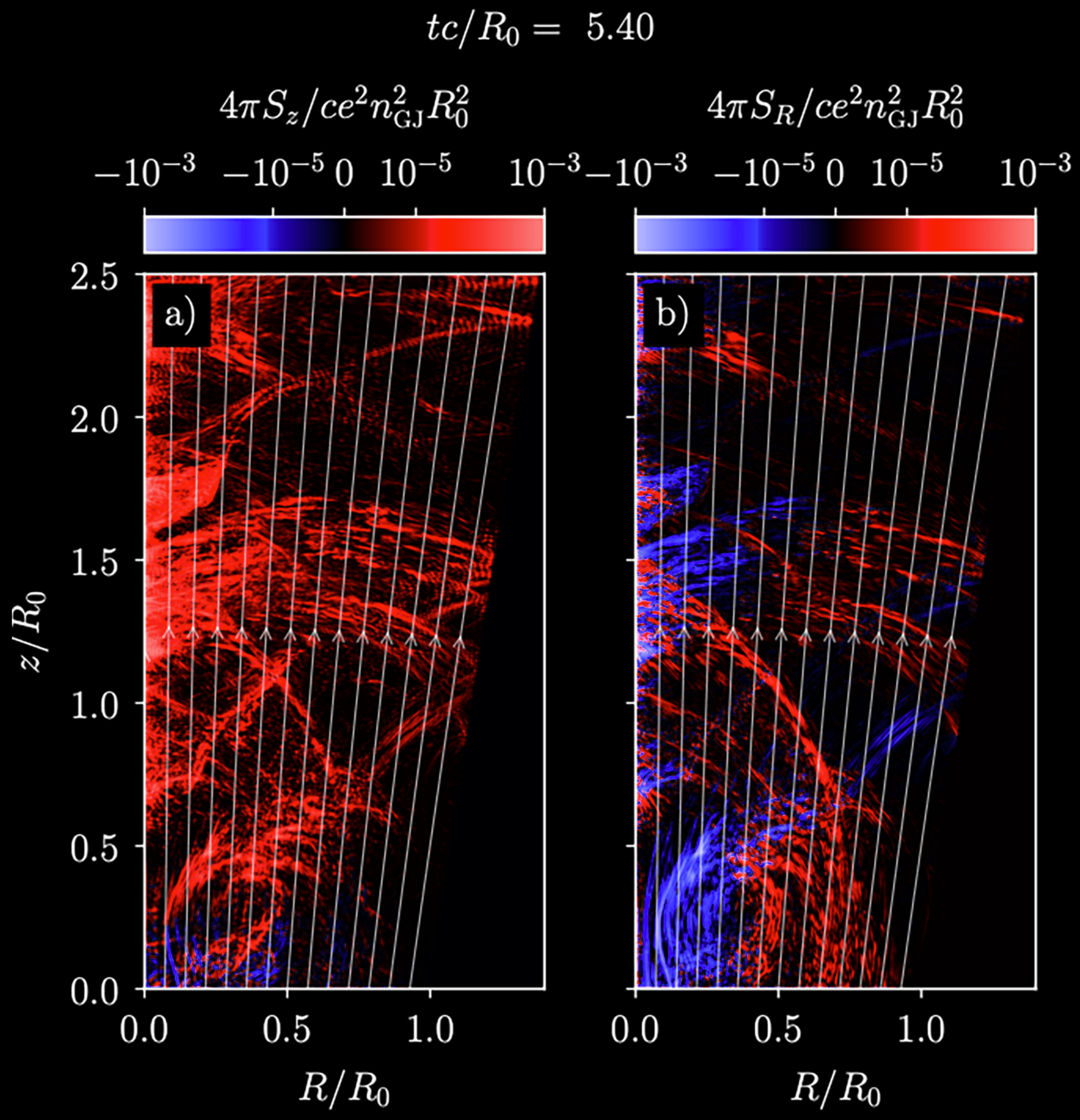

Cruz et. al., (2021) ApJL

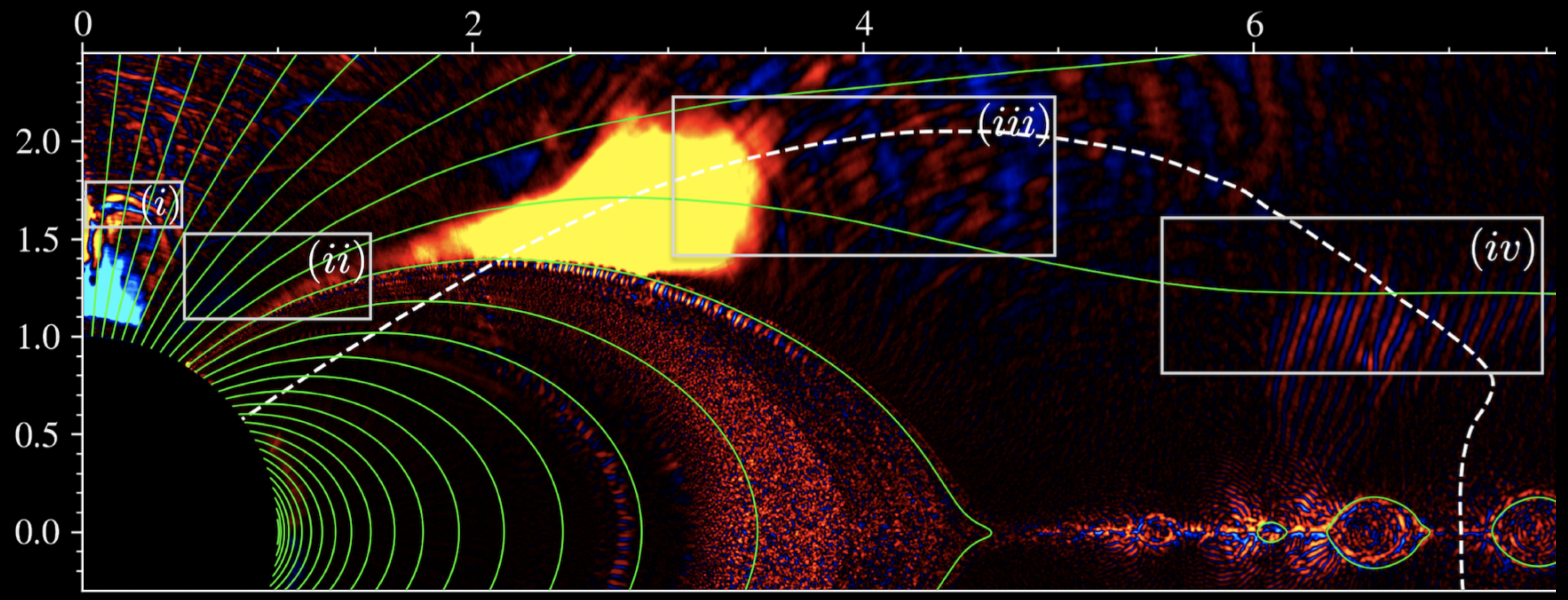

Bransgrove et. al., 2023, ApJL

Confirms order-of-magnitude luminosity

Core-cone geometry of the emission beam

PIC simulations with Osiris & Pigeon

CRAB RADIO EMISSION

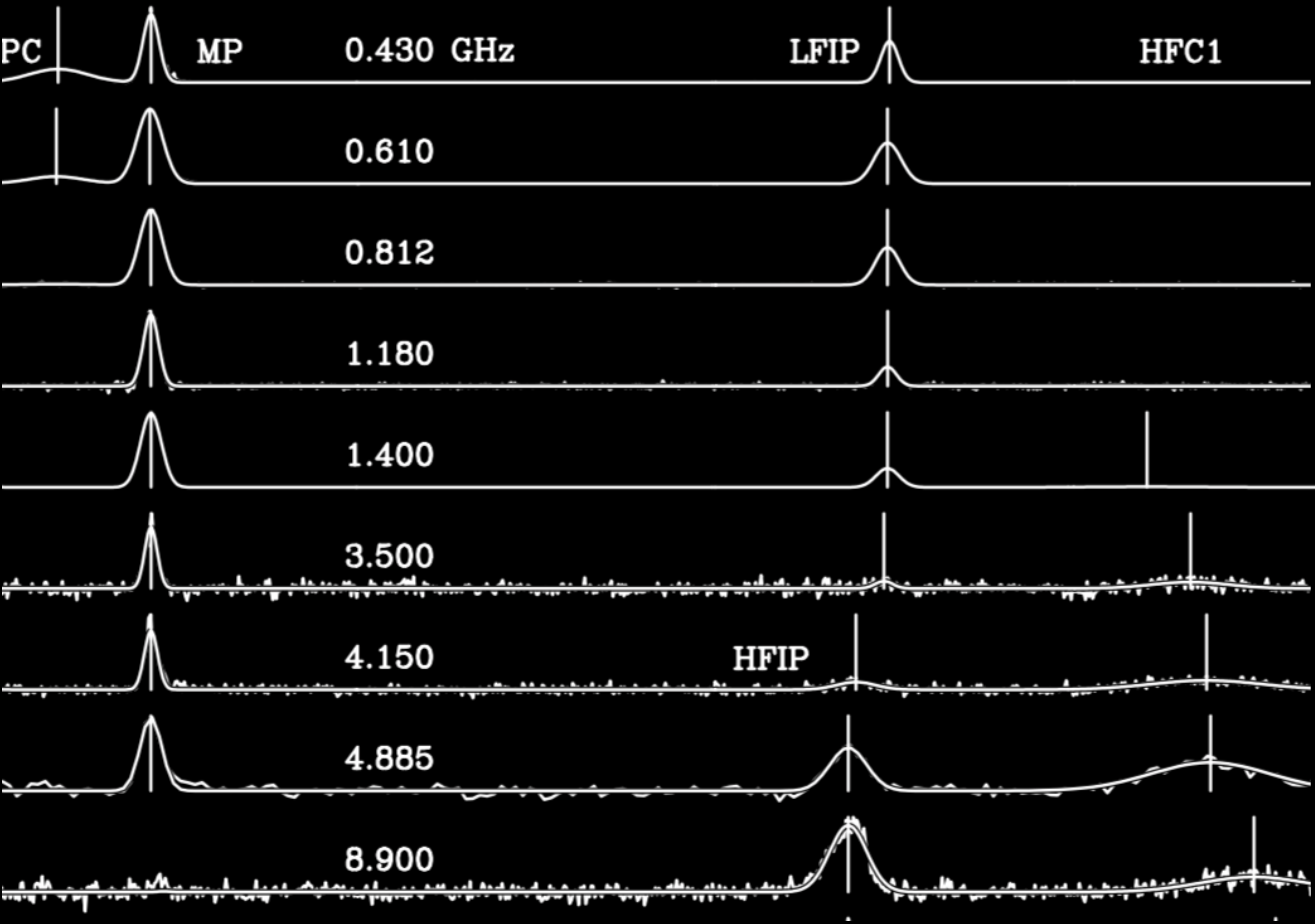

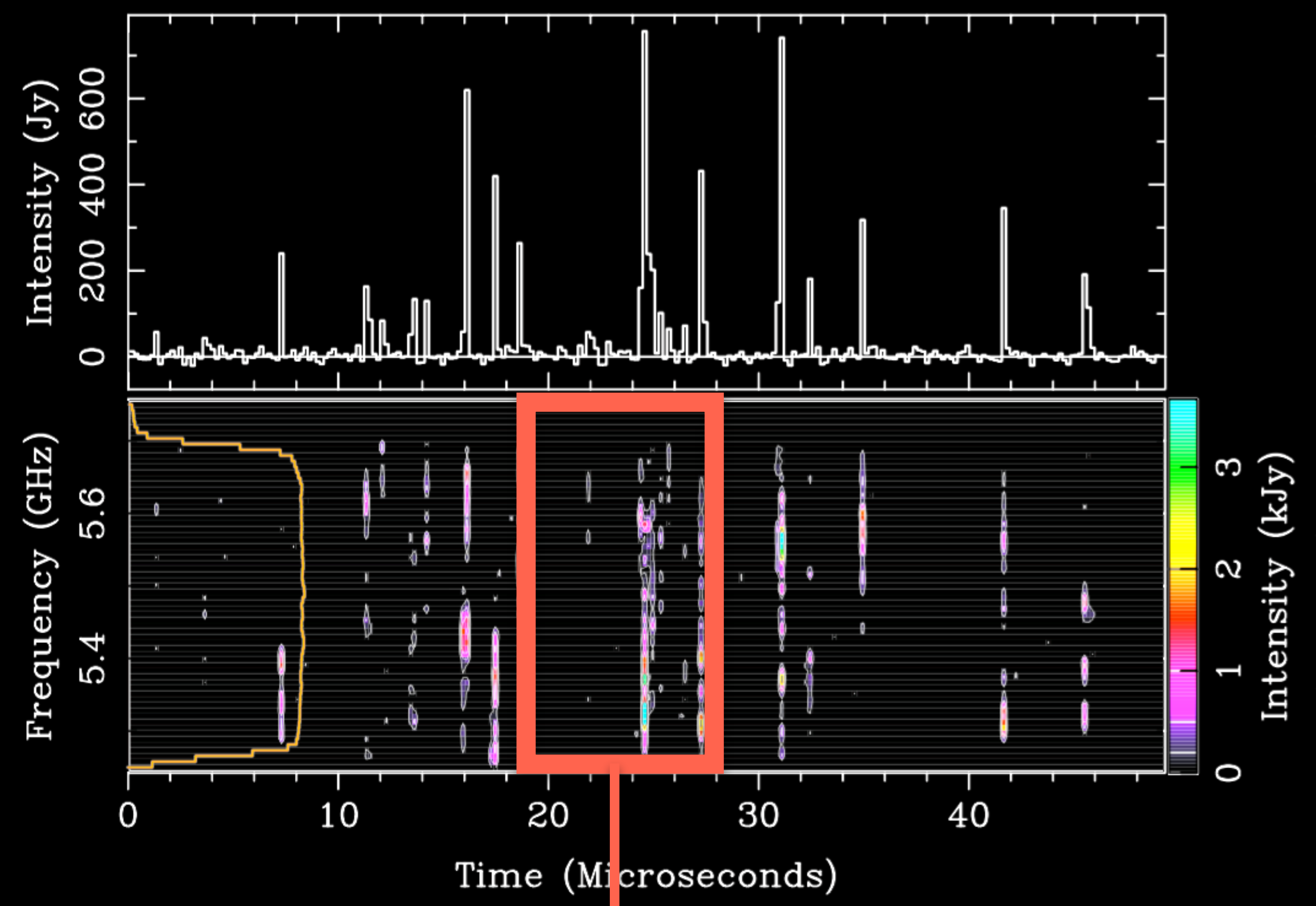

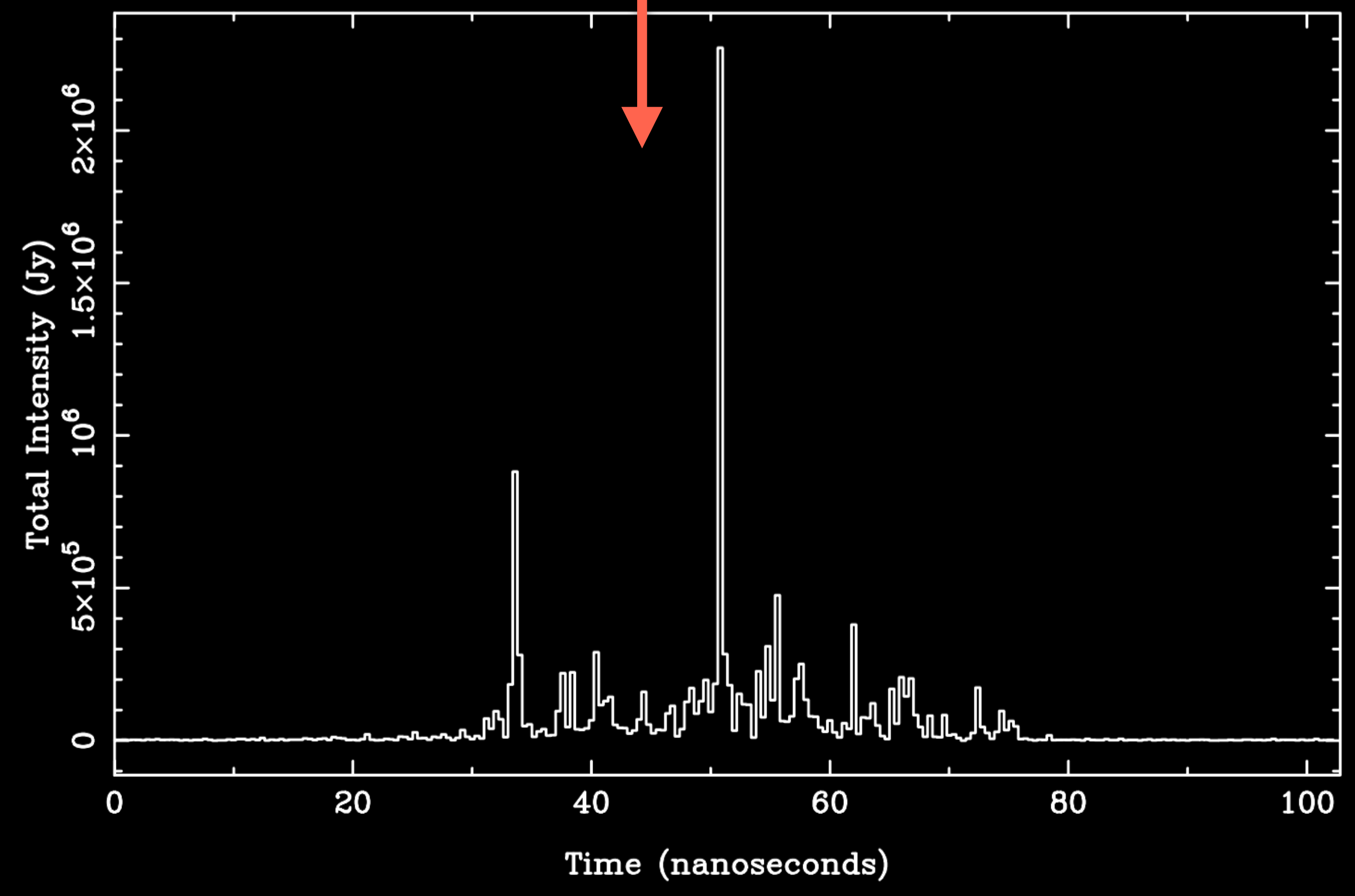

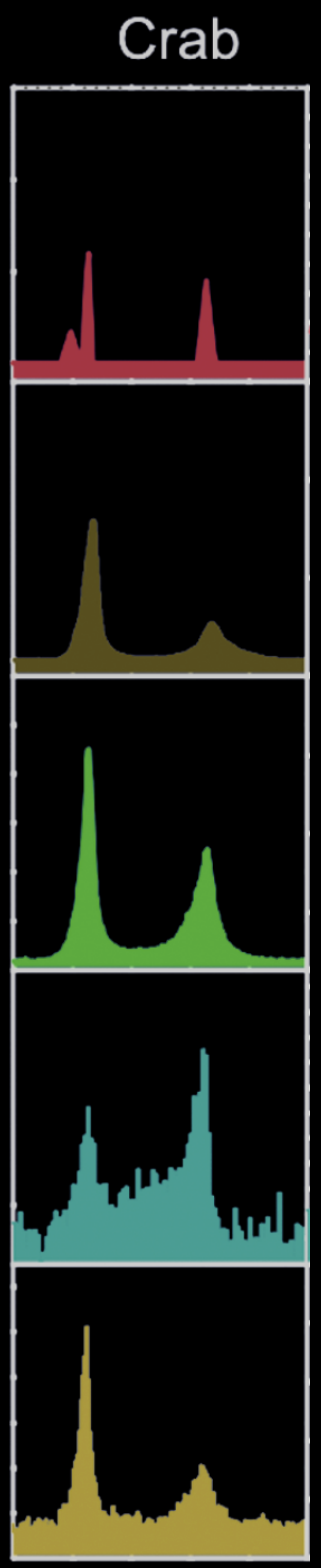

P ~ 33 ms

$$\nu_{\rm obs}\delta t \sim \mathcal{O}(10)$$

MP and IP have high-energy emission counter-parts ⇒ definitely originate from the outer magnetosphere

Hankins, Eilek, 2016 (JPP)

GIANT PULSES FROM RECONNECTION

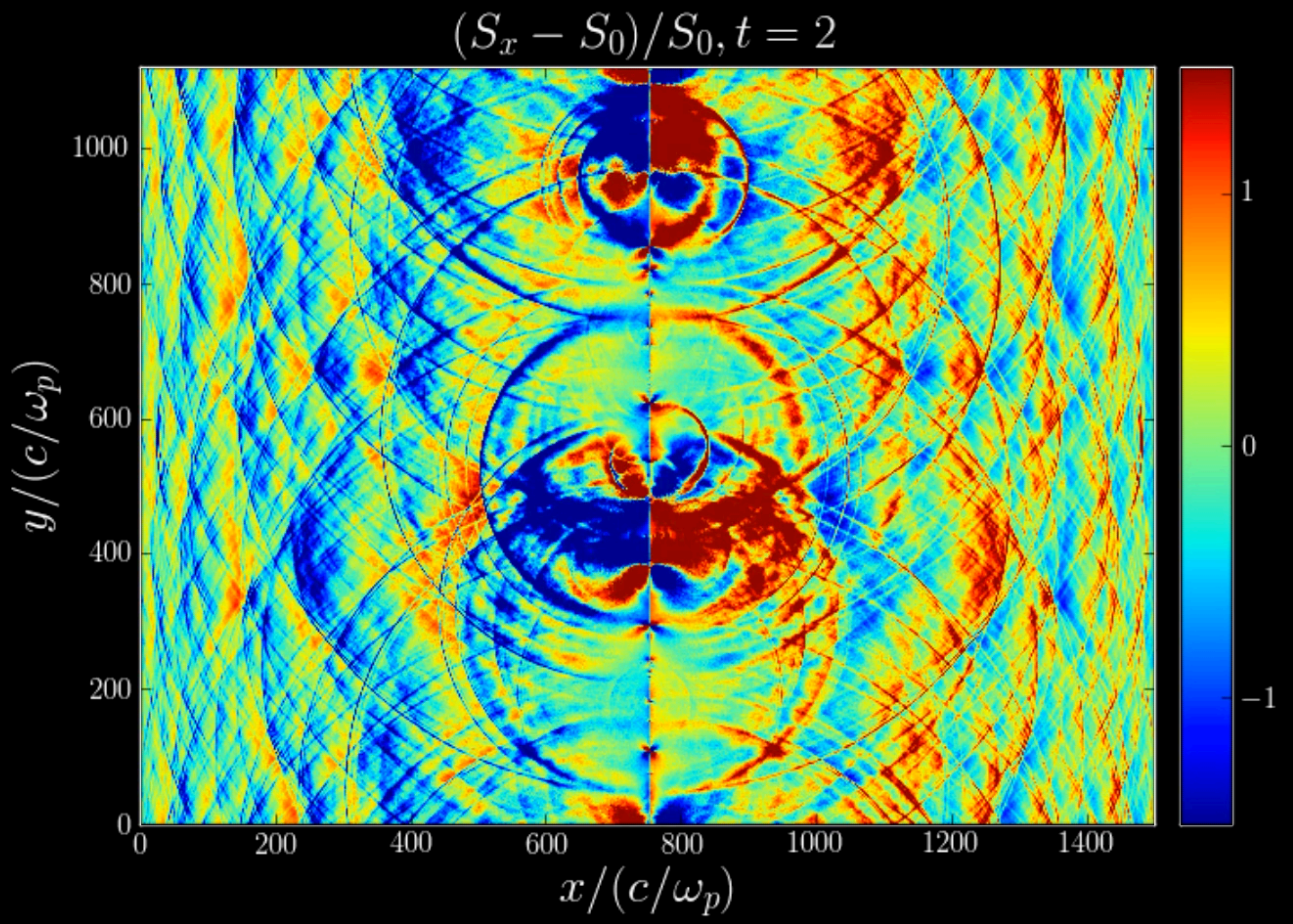

Philippov, Uzdensky, Spitkovsky, Cerutti, 2019 (ApJL)

- Current sheet breaks into plasmoids, plasmoids merge, EM waves are emitted.
- Amount of magnetic energy stored in a single plasmoid controls the brightness temperature. Can explain $T_{\rm B} \sim 10^{38}{\rm K}$!
- Plasmoid sizes set the frequency. Size is controlled by the strength of the radiative cooling, resulting in $\nu \sim c\Gamma/l \sim 1$ GHz $\cdot B_6^{3/2}$. Requires MGs B-field strength at the light cylinder. Mergers of big plasmoids produce pulses with duration $\tau \approx 10/\nu$.
- Prediction: some correlation with the X-rays, also produced by reconnection.
- Similar waves exist in 3D, work in progress.

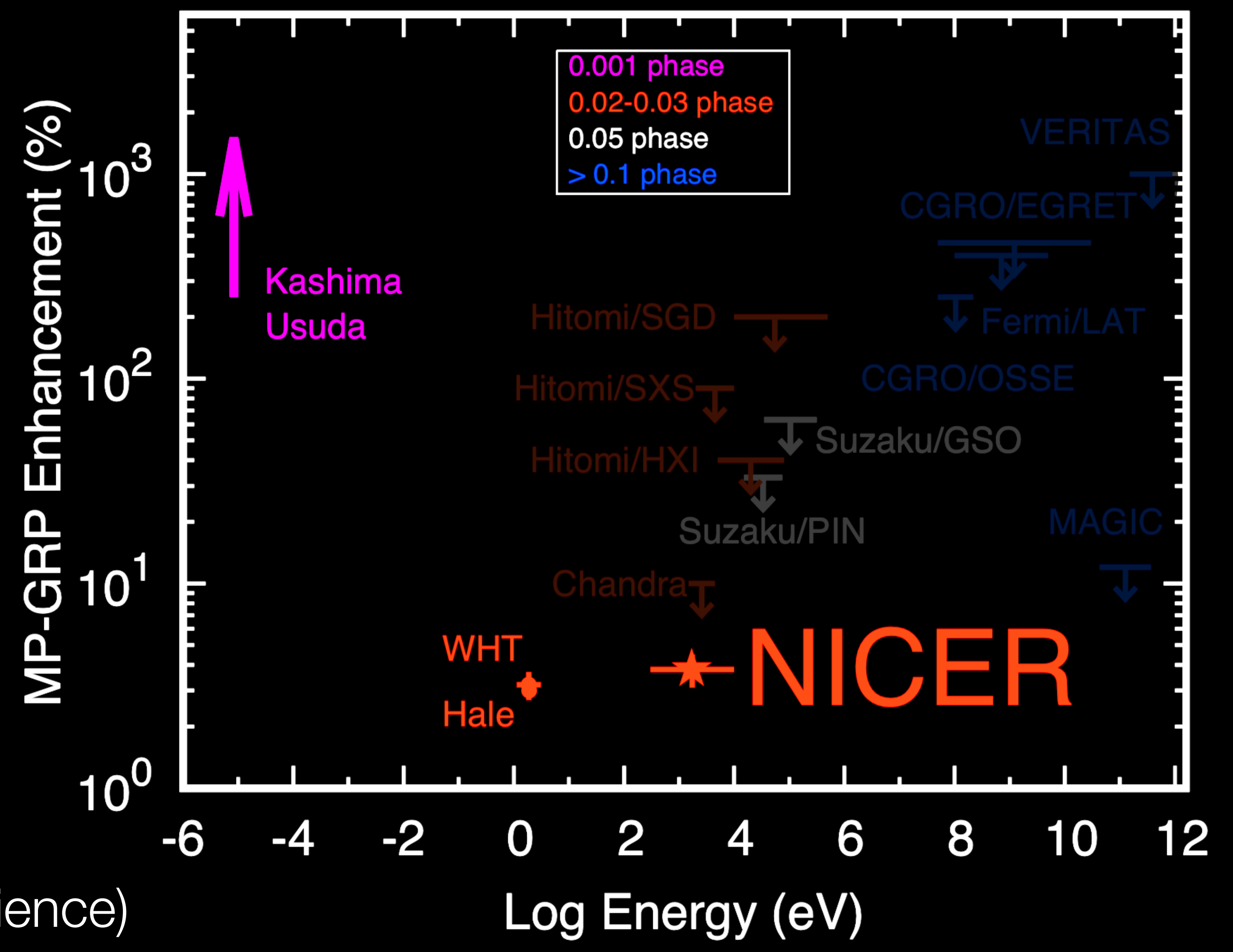

Enoto et. al., 2021 (Science)

Beyond Pulsars

Application to FRBs: magnetic explosions

Large eruptions

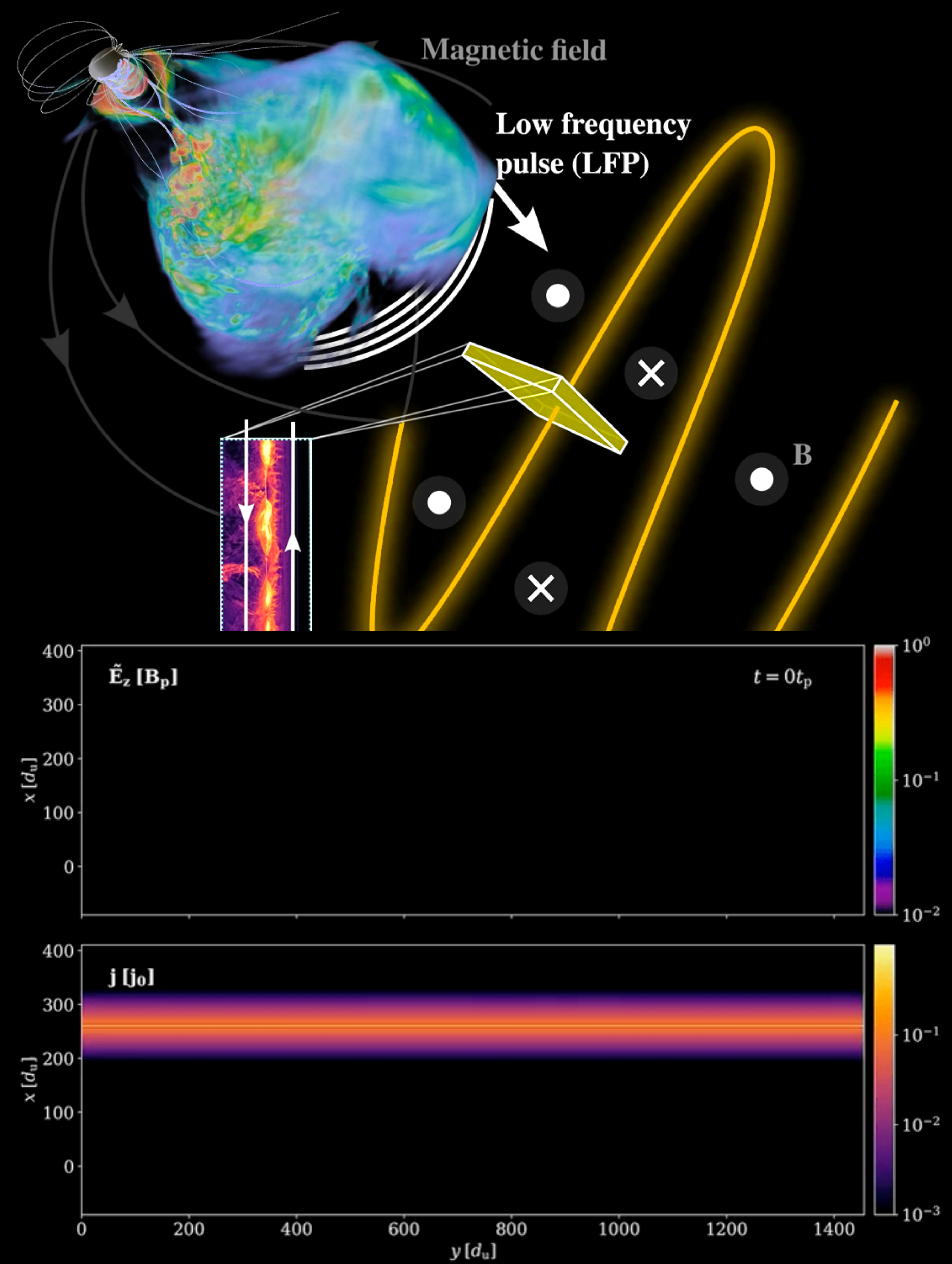

Mild eruptions

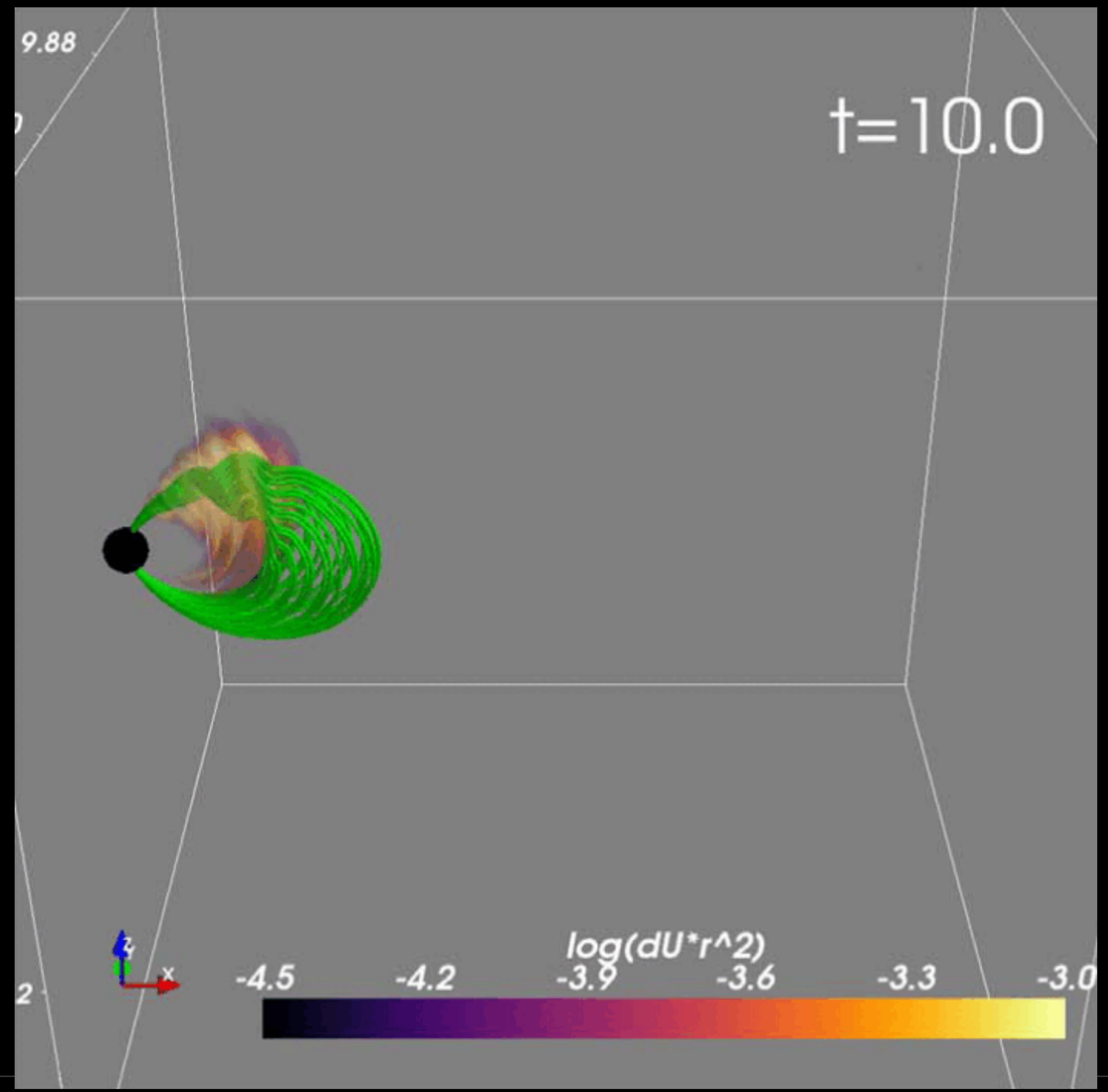

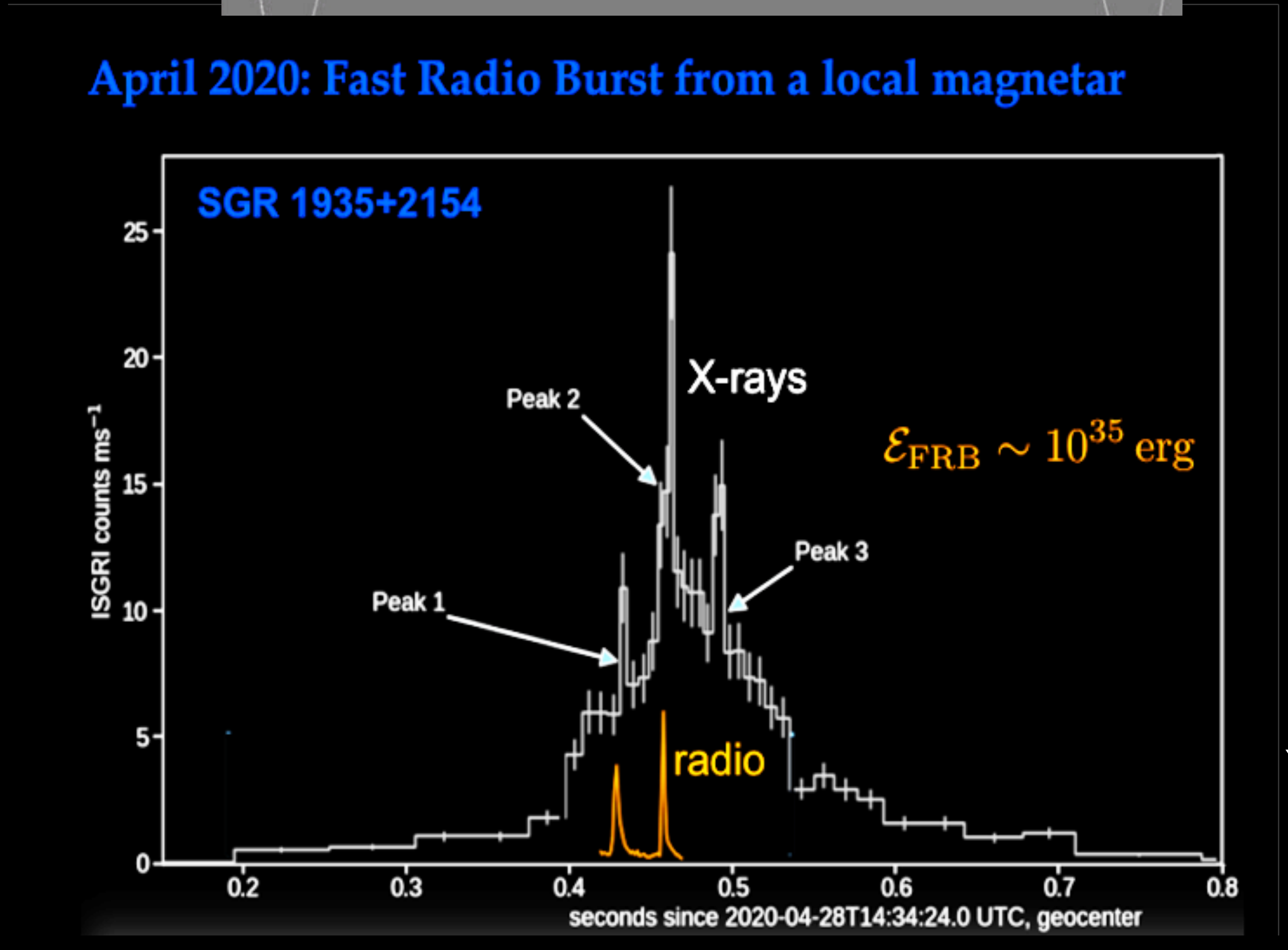

Potentially applicable to X-ray and FRB from galactic magnetar

Lyubarsky, 2020 (ApJ)
Mahlmann, Philippov et. al., 2022 (ApJL)
Yuan et. al. (including Philippov), 2022 (ApJ)

FRB / GP PROPAGATION

- High-amplitude FMS radiation is not free to leave.
- Quiescent magnetosphere: formation of shocks (Beloborodov 2023).
- More likely: surfing electromagnetic explosions.
- Non-linear wave interactions:
    - F <-> A+A
    - F <-> A+F

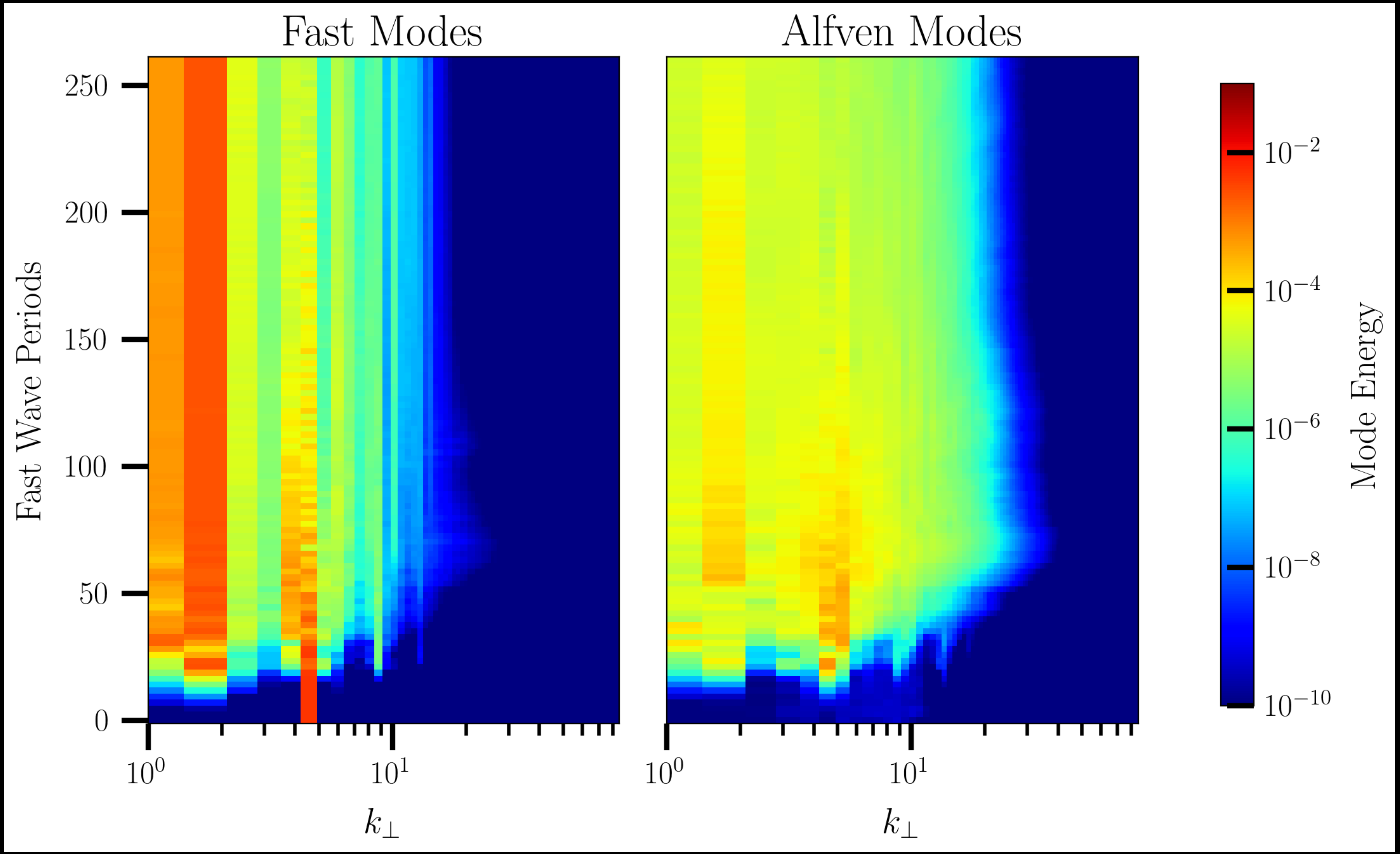

Future

- Pair production in 3D
- Old and Millisecond Pulsars
- Variability: nulling, thunderstorms, raindrops, drifting subpulses
- Other bands: optical, X-ray, etc.

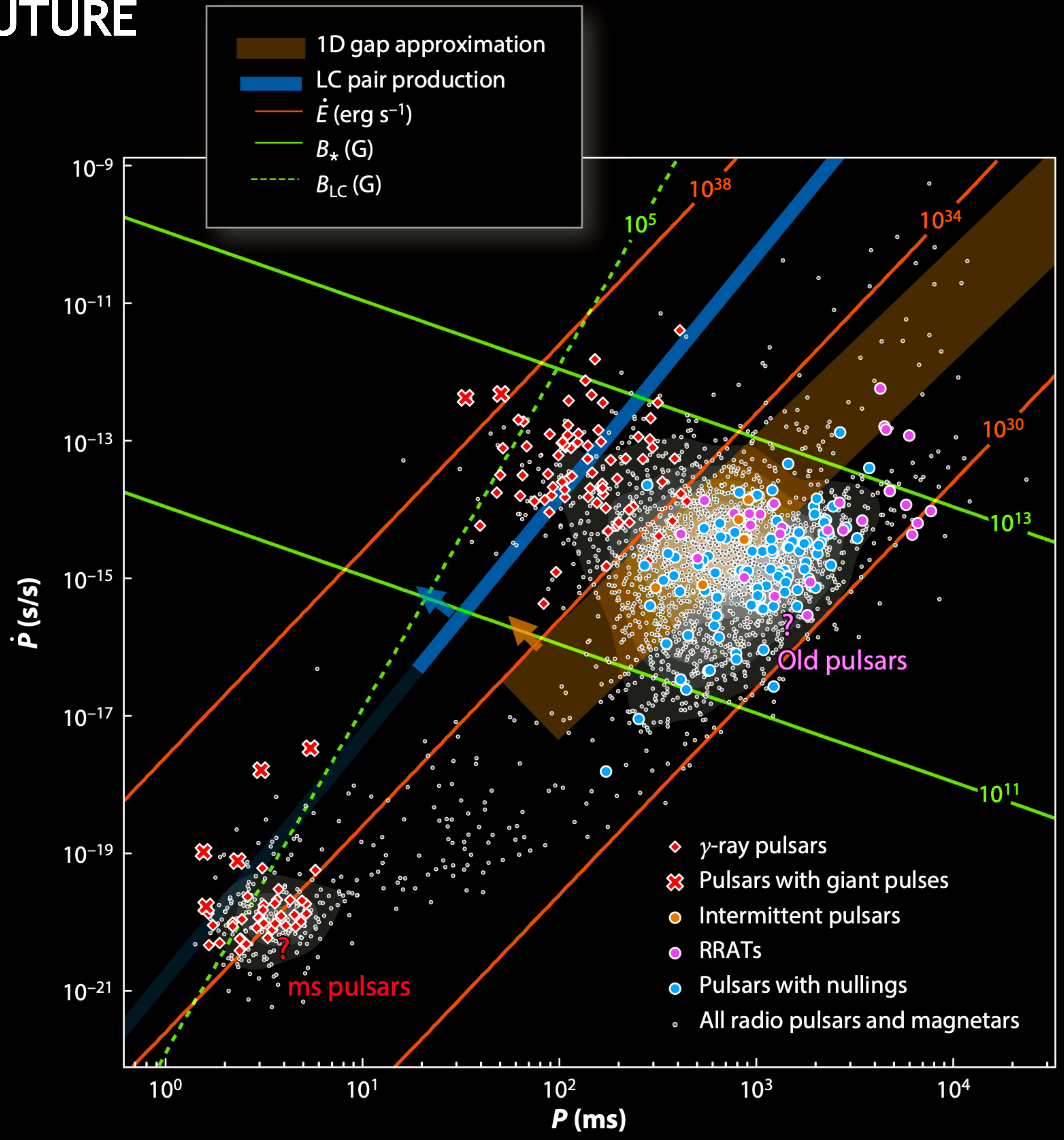

Future

- Pair production in 3D
- Old and Millisecond Pulsars
- Variability: nulling, thunderstorms, raindrops, drifting subpulses
- Other bands: optical, X-ray, etc.

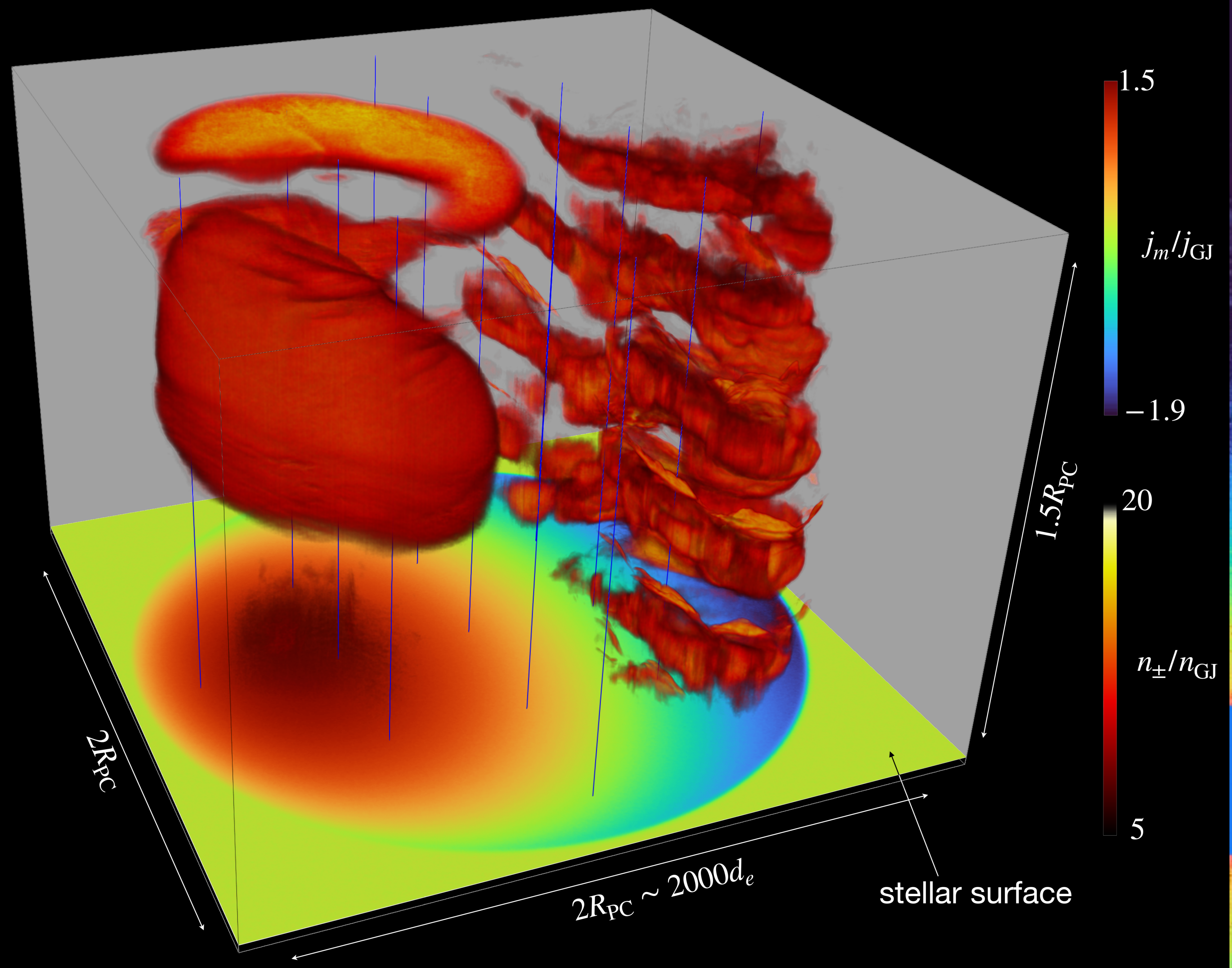

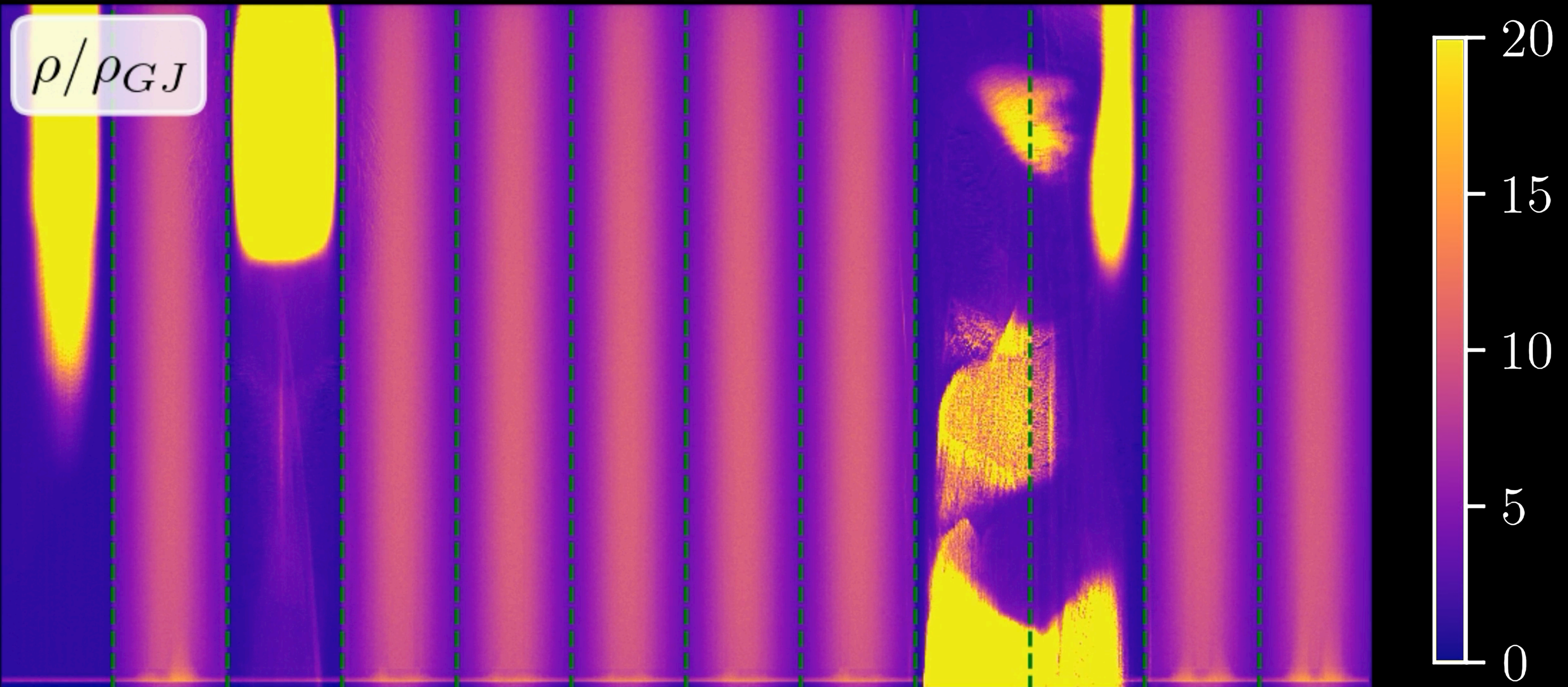

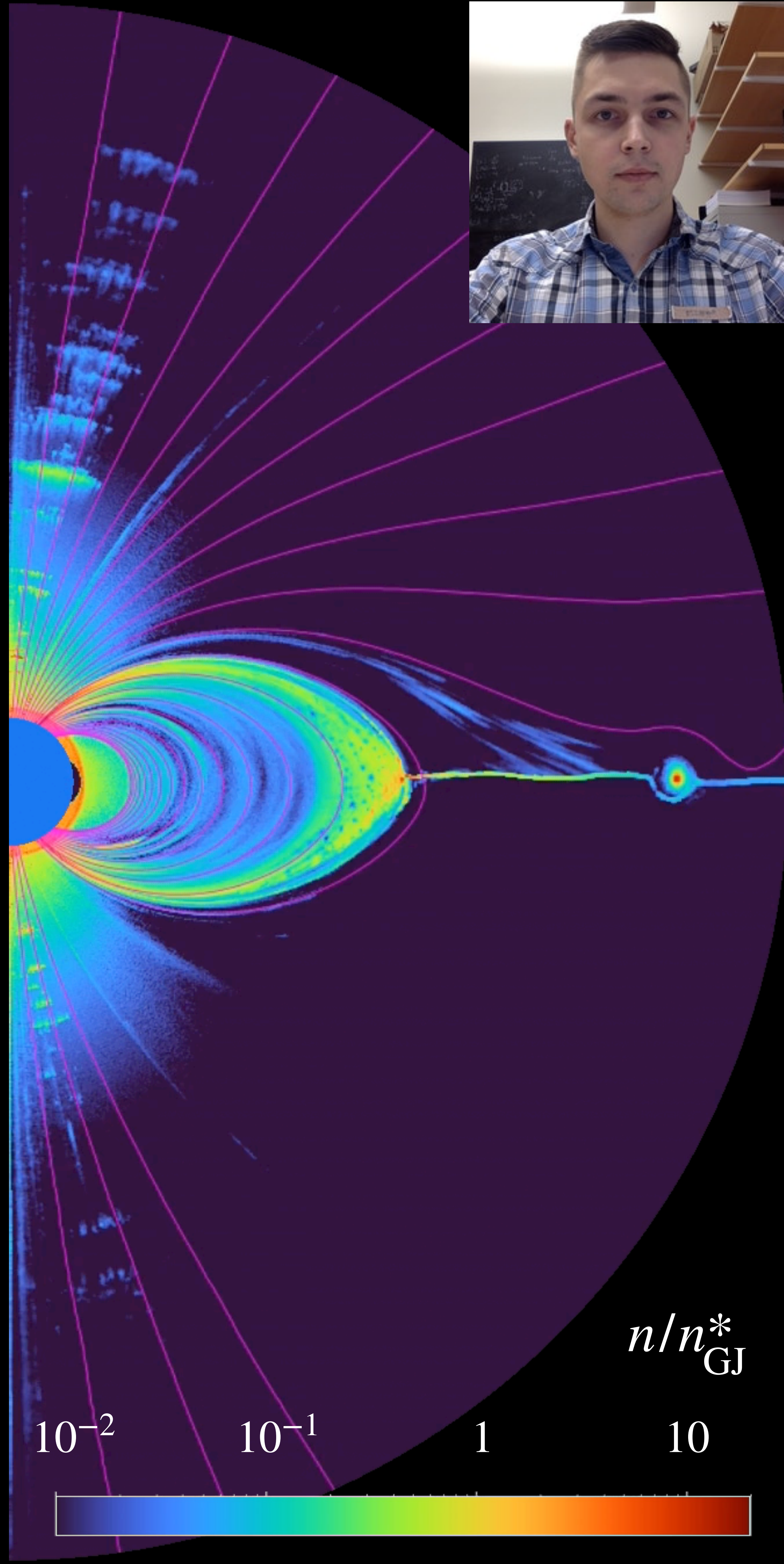

Magnetar Magnetospheres

- Ongoing: RICS pair-production
- Near-term: inclusion of QED processes for strong fields

Mahlmann, Philippov, Beloborodov et. al.

Conclusions and outlook

1. Origin of pulsar emission has been a puzzle since 1967 - kinetic plasma simulations are finally addressing this from first principles.

2. Current sheet is an effective particle accelerator. Particles in the sheet emit powerful gamma-ray mainly via synchrotron mechanism. Highest energy TeV photons can be produced in the current sheet as well.

3. Low altitute radio emission is produced during non-stationary discharge at the polar cap, not a plasma instability in the uniform plasma flow. Giant pulses and nanoshots are powered by plasmoid mergers in the currrent sheet beyond the light cylinder.

Pulsars and NICER

J0030+0451

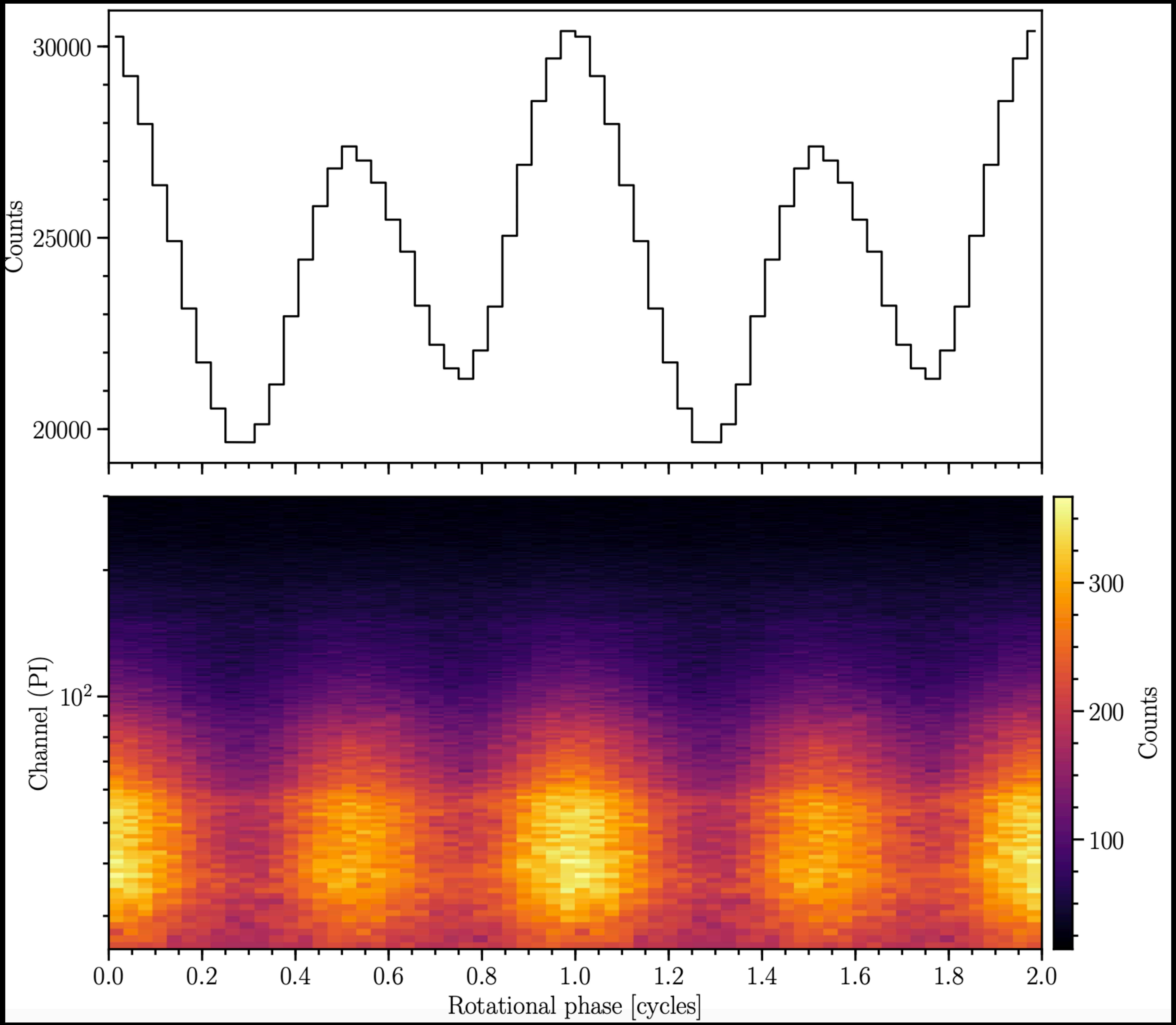

Riley et al., 2019

PULSARS AND NICER

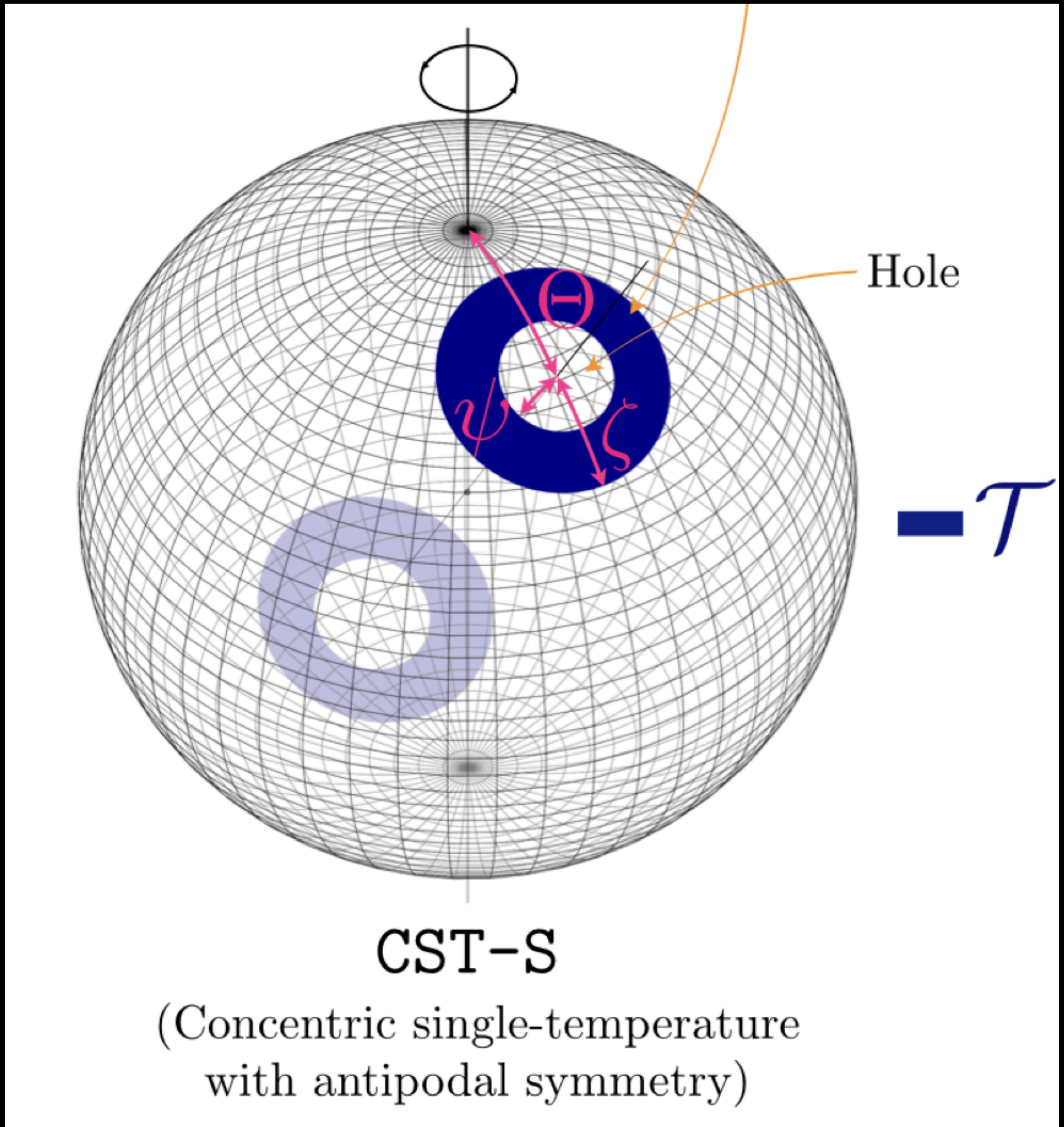

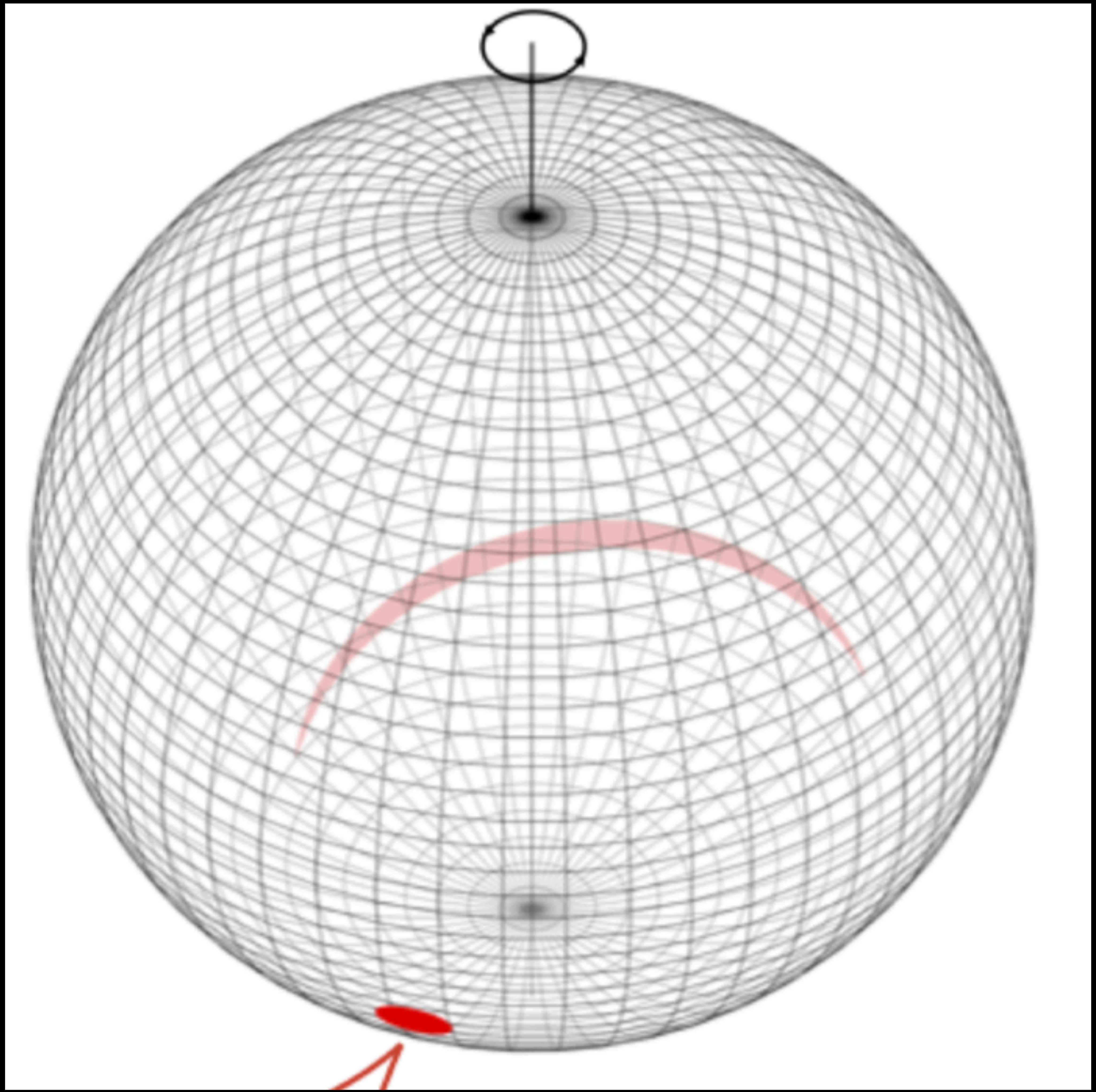

of parameters to describe. The inferred mass M and equatorial radius R_{eq} are, respectively, $1.34^{+0.15}_{-0.16}\,M_{\odot}$ and $12.71^{+1.14}_{-1.19}$ km, while the compactness $GM/R_{\text{eq}}c^2 = 0.156^{+0.008}_{-0.010}$ is more tightly constrained; the credible interval bounds reported here are approximately the 16% and 84% quantiles in marginal posterior mass.